© 2017. Published by The Company of Biologists Ltd | Journal of Cell Science (2017) 130, 1877-1889 doi:10.1242/jcs.201889

RESEARCH ARTICLE

SNAP-25 gene family members differentially support secretory vesicle fusion

Swati Arora, Ingrid Saarloos, Robbelien Kooistra, Rhea van de Bospoort, Matthijs Verhage* and Ruud F. Toonen*

ABSTRACT

Neuronal dense-core vesicles (DCVs) transport and secrete neuropeptides necessary for development, plasticity and survival, but little is known about their fusion mechanism. We show that *Snap-25*-null mutant (SNAP-25 KO) neurons, previously shown to degenerate after 4 days *in vitro* (DIV), contain fewer DCVs and have reduced DCV fusion probability in surviving neurons at DIV14. At DIV3, before degeneration, SNAP-25 KO neurons show normal DCV fusion, but one day later fusion is significantly reduced. To test if other SNAP homologs support DCV fusion, we expressed SNAP-23, SNAP-29 or SNAP-47 in SNAP-25 KO neurons. SNAP-23 and SNAP-29 rescued viability and supported DCV fusion in SNAP-25 KO neurons, but SNAP-23 did so more efficiently. SNAP-23 also rescued synaptic vesicle (SV) fusion while SNAP-29 did not. SNAP-47 failed to rescue viability and did not support DCV or SV fusion. These data demonstrate a developmental switch, in hippocampal neurons between DIV3 and DIV4, where DCV fusion becomes SNAP-25 dependent. Furthermore, SNAP-25 homologs support DCV and SV fusion and neuronal viability to variable extents – SNAP-23 most effectively, SNAP-29 less so and SNAP-47 ineffectively.

KEY WORDS: Neuropeptide vesicle, Fusion, SNAP-25, Hippocampal neuron

INTRODUCTION

Neuronal communication primarily relies on the Ca^{2+}-dependent fusion of two secretory organelles – synaptic vesicles (SVs) and neuropeptide-filled dense-core vesicles (DCVs). Neuropeptides modulate many aspects of brain function, including brain development, synaptogenesis, synaptic plasticity and survival (Huang and Reichardt, 2001; McAllister et al., 1999; Meyer-Lindenberg et al., 2011; Poo, 2001; Samson and Medcalf, 2015; van den Pol, 2012), and dysfunctional neuropeptide signaling is associated with several mood, anxiety and social disorders (reviewed in Kormos and Gaszner, 2013). However, in contrast to our in-depth understanding of SV fusion principles (for a review, see Südhof, 2013), much less is known about DCV transport and fusion mechanisms.

Soluble NSF attachment receptor (SNARE) proteins mediate membrane fusion of secretory vesicles (Ferro-Novick and Jahn, 1994). In neurons, the vesicular SNARE synaptobrevin-2 (also known as VAMP2) and membrane SNAREs syntaxin-1 and SNAP-25 drive fusion of SVs for fast neurotransmission (Jahn and Fasshauer, 2012; Südhof, 2013; Südhof and Rothman, 2009). Like SV fusion, DCV fusion is triggered by Ca^{2+} influx (Balkowiec and Katz, 2002; de Wit et al., 2009; Farina et al., 2015; Shimojo et al., 2015; van de Bospoort et al., 2012), although efficient DCV fusion typically requires more prolonged stimulation (Balkowiec and Katz, 2002; Bartfai et al., 1988; Hartmann et al., 2001; van de Bospoort et al., 2012). Neuronal DCVs are often highly mobile (de Wit et al., 2006; Wong et al., 2012), not pre-docked at their release sites (Hammarlund et al., 2008; van de Bospoort et al., 2012) and fuse at synaptic as well as extra-synaptic sites (de Wit et al., 2009; Hartmann et al., 2001; Ludwig and Leng, 2006; Matsuda et al., 2009). DCV fusion is sensitive to clostridial neurotoxins, indicating that neuropeptide release is SNARE dependent (de Wit et al., 2009; Hammarlund et al., 2008; McMahon et al., 1992; Shimojo et al., 2015). However, the composition of SNARE complexes that drive efficient DCV fusion in neurons is unknown.

The SNAP protein family comprises several homologous proteins, of which SNAP-25 is essential for SV fusion (Delgado-Martínez et al., 2007; Washbourne et al., 2002). Deletion of SNAP-25 leads to reduced neuronal survival and impaired arborization, reduced spontaneous release and arrest of evoked release in the surviving neurons (Delgado-Martínez et al., 2007). SNAP-23, the closest homolog of SNAP-25, is ubiquitously expressed and is involved in NMDA receptor cycling in post-synaptic spines (Suh et al., 2010). SNAP-23 overexpression rescues SV fusion in *Snap-25*-null mutant (SNAP-25 KO) neurons and secretory granule fusion in chromaffin cells, albeit with reduced efficiency (Sørensen et al., 2003; Delgado-Martínez et al., 2007). Two other SNAP family members, SNAP-29 and SNAP-47, are also present in neurons (Holt et al., 2006; Pan et al., 2005) and co-purify in synaptic vesicle purifications (Takamori et al., 2006). Overexpression of SNAP-29 inhibits synaptic vesicle fusion, possibly via inhibiting SNARE complex disassembly (Pan et al., 2005; Su et al., 2001). SNAP-47 binds to plasma membrane SNAREs *in vitro* but is predominantly located on intracellular membranes (Holt et al., 2006). Recent data has shown that shRNA-mediated knockdown of SNAP-25 or SNAP-47 expression interferes with Ca^{2+}-dependent release of brain-derived neurotrophic factor (BDNF) in cortical neurons (Shimojo et al., 2015).

Here, we investigated the role of SNAP-25 in DCV fusion in cultured hippocampal neurons at 3-4 days *in vitro* (DIV; before synapse formation) and at DIV14 after synapses are formed. We find that neuronal DCV fusion is strongly impaired in SNAP-25 KO neurons at DIV14 but that Ca^{2+}-evoked fusion at DIV3, but not DIV4, is SNAP-25 independent. In addition, we show a differential ability of SNAP-25 family members to support neuronal viability, and DCV and SV fusion in SNAP25 KO neurons at DIV14.

Department of Functional Genomics and Clinical Genetics, Center for Neurogenomics and Cognitive Research, Neuroscience Campus Amsterdam, Vrije Universiteit (VU) Amsterdam and VU Medical Center, de Boelelaan 1085, Amsterdam 1081 HV, The Netherlands.

*Authors for correspondence (matthijs.verhage@cncr.vu.nl; ruud.toonen@cncr.vu.nl)

S.A., 0000-0002-9442-3359; R.K., 0000-0003-4576-8964; M.V., 0000-0002-2514-0216; R.F.T., 0000-0002-9900-4233

Received 26 January 2017; Accepted 9 April 2017

Journal of Cell Science (2017) 130, 1877-1889 doi:10.1242/jcs.201889

RESULTS

SNAP-25 is required for efficient DCV fusion in DIV14 neurons

To investigate the role of SNAP-25 in neuronal DCV fusion, we first analyzed the effect of SNAP-25 deletion on survival and morphology of single isolated hippocampal neurons of SNAP-25 KO mice (Washbourne et al., 2002) and wild-type (WT) littermates (Fig. S1A). In line with previous reports (Delgado-Martínez et al., 2007; Washbourne et al., 2002), the majority (approximately 98%) of SNAP-25 KO neurons did not survive beyond DIV4 in culture (Fig. S1B). At DIV14, the surviving SNAP-25 KO neurons had smaller dendrites and axons, contained fewer VGLUT1- or synaptophysin-labeled synapses and DCVs compared with WT littermates (Fig. 1A; Fig. S1A-M for quantification). In our culture system, the majority of neurons were glutamatergic, and SNAP-25 deletion did not affect the ratio of glutamatergic (VGLUT1-positive) over GABAergic (VGAT-positive) neurons at DIV14 (WT: 12.4% GABAergic; SNAP-25 KO 15.1% GABAergic; Mann–Whitney test, P=0.32). Next, we expressed pHluorin-

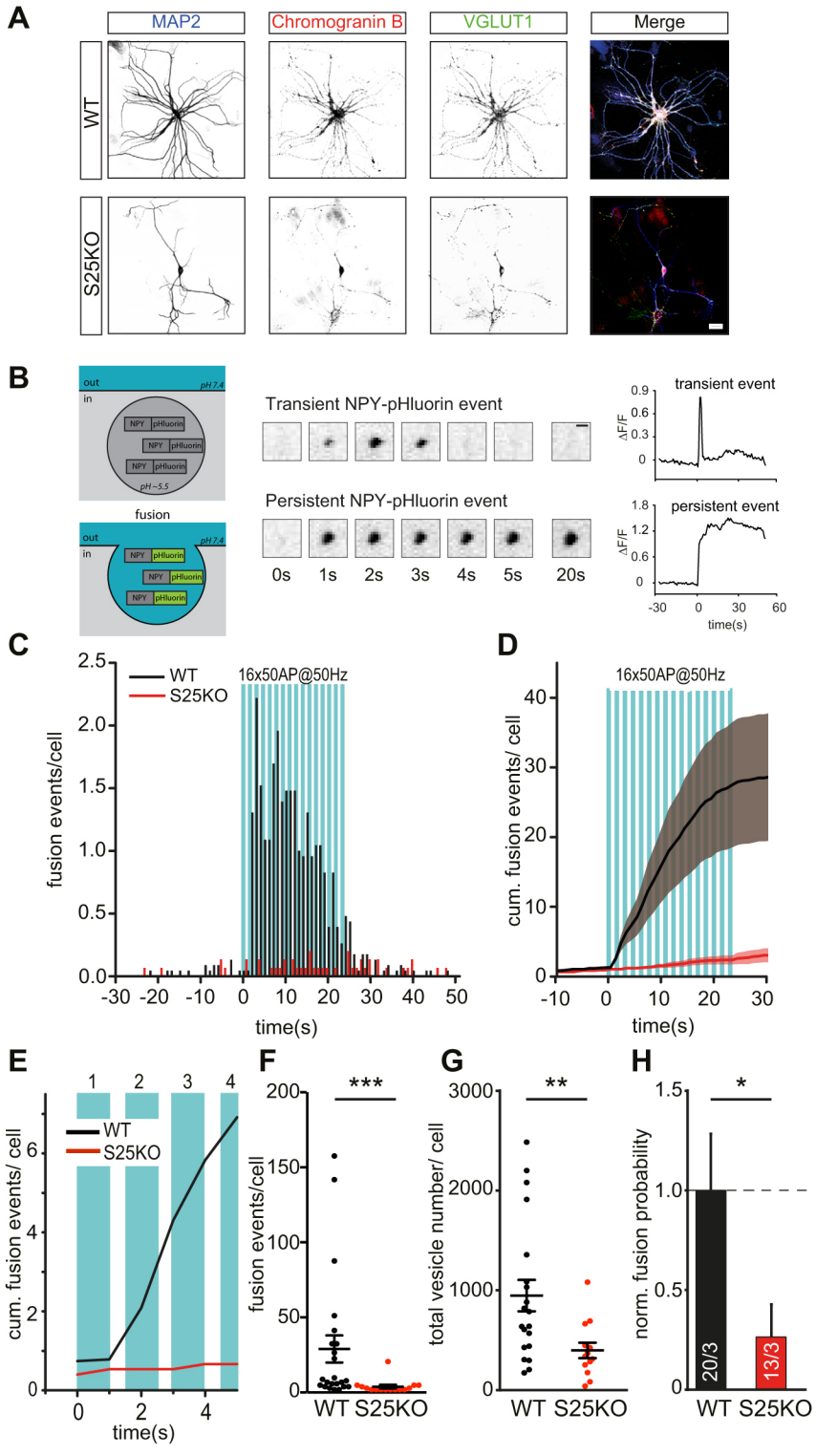

Fig. 1. Impaired DCV fusion in DIV14-21 SNAP-25 KO neurons. (A) Representative images of single isolated SNAP-25 KO (S25KO) and WT neurons stained for the dendritic marker MAP2 (blue), endogenous DCV marker chromogranin B (red) and glutamatergic synapse marker VGLUT1 (green). Scale bar: 25 µm. See Fig. S1 for quantification of morphology. (B) Schematic diagram of a DCV labeled with NPY–pHluorin. NPY–pHluorin fluorescence is quenched in the acidic lumen of a DCV. Upon fusion, the pH instantly rises and de-quenches NPY–pHluorin. Representative examples of Ca^{2+}-dependent NPY–pHluorin fusion events categorized as transient and persistent based upon duration of the fluorescence signal. Stills show sudden increases and rapid decreases of NPY–pHluorin fluorescence (upper panels, transient event) and sudden increase followed by prolonged fluorescence (lower panels, persistent event). Panels on the right show ΔF/F0 traces of transient or persistent events. Both types of events were included in the analysis of DCV fusion. (C) Histogram of fusion events from control (WT) and SNAP-25 KO (S25KO) neurons before, during and after stimulation. Stimulation comprised 16 bursts of 50 APs at 50 Hz (16×50AP@50 Hz) represented by blue bars. WT neurons showed robust DCV fusion after the first AP burst while fusion in SNAP-25 KO neurons was strongly impaired. (D) Mean cumulative (cum.) frequency of DCV fusion events per cell before, during and after stimulation. (E) Mean cumulative frequency of fusion events during the first four bursts of 50 APs at 50 Hz shows that DCV fusion starts after the first AP burst in WT but not in SNAP-25 KO neurons. (F) Mean number of DCV fusion events per cell for WT and S25KO neurons (WT: n=20 cells, N=3 independent experiments, 657 events; S25KO: n=13 cells, N=3, 47 events; Mann–Whitney, ***P<0.001). (G,H) Total DCV number, measured upon dequenching of NPY–pHluorin using 50 mM NH_4^+ superfusion, and fusion probability are strongly reduced in SNAP-25 KO neurons. (G) Mean total DCV number per cell in WT and S25KO neurons (WT: n=20 cells, 18929 vesicles; S25KO: n=13 cells, 5147 vesicles; Mann–Whitney, **P=0.009). (H) Normalized DCV fusion probability (NFP) during stimulation in WT and S25KO neurons. (WT: n=20 cells, NFP=1.0; S25KO: n=13 cells, NFP=0.2692; Mann–Whitney, *P=0.0192). Data is plotted as mean±s.e.m. Dots in 1F,G represent individual neurons. Numbers in bars on H represent number of cells/number of independent experiments.

Journal of Cell Science (2017) 130, 1877-1889 doi:10.1242/jcs.201889

tagged neuropeptide Y (NPY–pHluorin), a DCV cargo reporter that allows analysis of DCV fusion events with single-vesicle resolution. A rapid increase in fluorescence is detected upon pHluorin de-quenching when the fusion pore opens, and this is followed by a rapid decline of fluorescence (transient event, representing full release of cargo or endocytosis and DCV re-acidification) or prolonged fluorescence (persistent event, representing prolonged fusion pore opening or stable deposits of NPY–pHluorin at the membrane), which is typical for neuronal DCV fusion (Fig. 1B; de Wit et al., 2009; Farina et al., 2015; van de Bospoort et al., 2012). In WT cells, bursts of action potentials (APs) (16 bursts of 50 AP at 50 Hz, Farina et al., 2015; Hartmann et al., 2001; van de Bospoort et al., 2012) triggered robust DCV fusion (28.6±9.2 events/cell; mean±s.e.m.; Fig. 1C,F). In contrast, SNAP-25 KO neurons showed a more than ninefold reduction in DCV fusion events upon stimulation (3.1±1.3 events/cell, Fig. 1C,F). Deletion of SNAP-25 equally affected DCV fusion at synaptic and extra-synaptic sites (Fig. S1N,O). WT cells showed a sharp increase in DCV fusion events after the first burst of 50 APs (Fig. 1D). In contrast, DCV fusion in SNAP-25 KO neurons required more prolonged stimulation and never reached the fusion rates observed in WT cells (Fig. 1D,E).

To test if the smaller size of SNAP-25 KO neurons resulted in a reduced total number of DCVs, we quantified the number of DCV puncta upon instant de-quenching of intravesicular NPY–pHluorin using NH_4Cl superfusion (de Wit et al., 2009). The total number of NPY–pHluorin puncta was >50% lower in SNAP-25 KO neurons compared with WT (Fig. 1G, WT: 974.6±157.6, n=20; SNAP-25 KO: 399.2±78.2, n=13). The DCV fusion probability, defined as the number of fusion events/total DCV number per cell, was strongly reduced in SNAP-25 KO neurons (Fig. 1H). Hence, SNAP-25 is critical for efficient stimulation-dependent DCV fusion in DIV14 hippocampal neurons. Its absence results in reduced DCV numbers and fusion probability, also after correcting for the smaller size of SNAP-25 KO neurons.

DCV fusion is Ca^{2+} dependent at DIV3 but becomes SNAP-25 dependent only at DIV4

SNAP-25 KO neurons show signs of degeneration at 3-4 DIV, and >98% of these neurons do not survive beyond DIV8 (Fig. S1B; Delgado-Martínez et al., 2007; Washbourne et al., 2002). To test if reduced release of neuropeptides and neurotrophic factors may help to explain this phenotype, we first assessed whether our functional DCV probe NPY–pHluorin also labels DCVs in developing neurons by analyzing its colocalization with the endogenous DCV cargo secretogranin II (SecgrII; Bartolomucci et al., 2011) at DIV4. Both Pearson's and Manders' coefficients confirmed robust colocalization of NPY–pHluorin and SecgrII at DIV4, similar to colocalization of NPY–pHluorin with SecgrII or ChgB at DIV14 (Fig. 2B,C), indicating that our probe is correctly targeted to DCVs in developing neurons. Next, using NPY–pHluorin, we examined DCV fusion in neurons at DIV3 and DIV4, at which time neurons develop extensive axonal and dendritic arborizations *in vitro* and expression levels of SNAP-25 strongly increase (Fig. 2A; Fig. S2J,K). At both time points, SNAP-25 KO neurons had smaller neurites with less complex arborization compared with WT neurons (Fig. S2A-H). AP stimulation resulted in a robust increase in intracellular Ca^{2+} (Fig. 2D,E, insets). In DIV3 neurons, stimulation failed to elicit fusion in approximately 60% of WT and SNAP-25 KO neurons (Fig. S2I), but events were observed in the other 40%. These events were stimulus dependent in both genotypes (Fig. 2D), and similar between WT and SNAP-25 KO neurons (Fig. 2D,F,G). The number of DCV fusion events at DIV3 was almost tenfold lower than at DIV14 (compare Fig. 2F with Fig. 1F). At DIV4, a larger fraction of neurons responded to AP stimulation (Fig. S2I), and more DCV fusion events were observed in WT neurons than were observed at DIV3 (Fig. 2E,F,H). However, fusion events were less frequent and more asynchronous in response to the same stimulation in SNAP-25 KO neurons (Fig. 2E,H). Hence, while at DIV3 WT and SNAP-25 KO neurons responded in a similar manner to stimulation, at DIV4, SNAP-25 KO neurons were clearly impaired.

The total number of NPY–pHluorin-labeled DCVs, assessed upon brief superfusion with NH_4^+, in SNAP-25 KO neurons was somewhat lower but not statistically different than in WT neurons both at DIV3 and DIV4 (Fig. 2I). To correct for the total vesicle pool between the two genotypes, we computed the DCV fusion probability – i.e. the number of fusion events divided by the total number of vesicles per neuron. The fusion probability was similar between the genotypes at DIV3 (Fig. 2J), but lower in SNAP-25 KO neurons at DIV4 (Fig. 2K). In conclusion, activity-dependent DCV fusion was reduced at DIV4, but not at DIV3, in SNAP-25 KO neurons. Hence, DCV fusion appears to become SNAP-25 dependent between DIV3 and DIV4, coinciding with a reduction of SNAP-23 expression in SNAP-25 KO neurons (Fig. S2L) and the occurrence of cell death.

SNAP-23 and SNAP-25, but not SNAP-29, rescue synaptic vesicle fusion capacity in SNAP-25 KO neurons at DIV14

Re-expression of SNAP-25 rescues neuronal viability and neurotransmission in SNAP-25 KO hippocampal neurons (Delgado-Martínez et al., 2007). To test if, and to what extent, other SNAP-25-related genes can rescue neuronal viability and SV fusion, we expressed SNAP-23, SNAP-29 or SNAP-47 using lentiviral infections in SNAP-25 KO neurons (Fig. S3A-C). Viral expression of SNAP-23 or SNAP-29 resulted in an approximately twofold increase in cellular protein levels (Fig. S3S-U). Expression of these proteins rescued neuronal viability, similar to SNAP-25 expression. Dendrite morphology and synapse number were comparable between SNAP-25 KO neurons expressing SNAP-23 or SNAP-25, but SNAP-29-expressing SNAP-25 KO neurons were smaller and had fewer synapses (Fig. S3D-R). The synapses of the few SNAP-25 KO neurons that survived until DIV14 showed a higher expression level of endogenous SNAP-23, but not SNAP-29, as compared to WT neurons (Fig. 3A). Viral expression at DIV1 further increased the mean synaptic levels of SNAP-23 or SNAP-29 in SNAP-25 KO neurons, whereas SNAP-25 expression produced synaptic protein levels almost similar to those of WT neurons (Fig. 3A). SNAP-47 did not rescue viability of SNAP-25 KO neurons, despite the fact that viral expression of SNAP-47 resulted in a twofold increase compared to endogenous SNAP-47 expression levels (see below).

Next, we assessed SV fusion using the synaptic vesicle protein synaptophysin fused to a pH-sensitive fluorophore (pHluorin) in a luminal domain (SypHy, Granseth et al., 2006). As expected, APs (200 APs at 10 Hz) did not elicit SV fusion in SNAP-25 KO neurons (Fig. 3C-F). Expression of SNAP-23 or SNAP-25 restored SV fusion capacity in 90-100% of SNAP-25 KO neurons. In contrast, although expression of SNAP-29 rescued survival, AP-triggered fusion events were not detected in these cells (Fig. 3C). The total SV pool, assessed by brief superfusion of NH_4^+, was smaller in SNAP-29-rescued neurons compared with WT neurons, but larger than in SNAP-25 KO neurons (Fig. 3D). The SV fusion probability in SNAP-25 KO neurons expressing SNAP-23 was not significantly

Journal of Cell Science (2017) 130, 1877-1889 doi:10.1242/jcs.201889

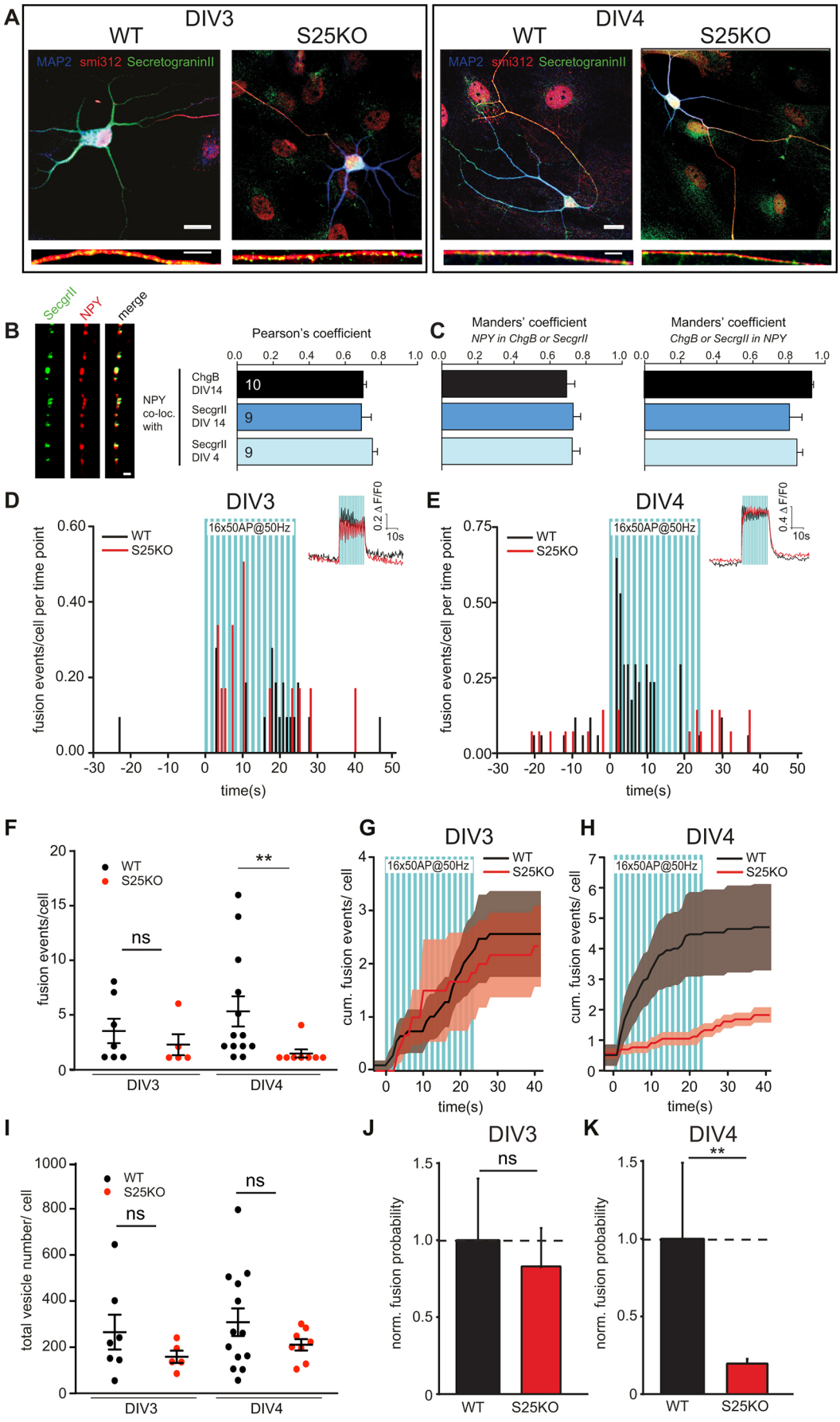

Fig. 2. See next page for legend.

Journal of Cell Science (2017) 130, 1877-1889 doi:10.1242/jcs.201889

Fig. 2. Ca^{2+}- and SNAP-25-dependent DCV fusion in DIV3 and DIV4 neurons. (A) Representative images of single isolated SNAP-25 KO and WT neurons at DIV3 (left) and DIV4 (right) stained for dendritic MAP2, the axonal smi312 antibody and endogenous DCV marker secretogranin II (SecgrII). Scale bars: 15 µm (DIV3, DIV4), 4 µm (DIV3 zoom); 3 µm (DIV4 zoom). (B) Representative image of DIV4 neurite showing colocalization (co-loc.) of NPY–pHluorin (stained with EGFP antibody) and endogenous SecgrII. Colocalization analysis of overexpressed NPY–pHluorin with SecgrII at DIV14 and DIV4, and with chromogranin B (ChgB) at DIV14 in neurons, quantified using Pearson's coefficient. (C) Manders' coefficient for the overlap of overexpressed NPY–pHluorin with endogenous SecgrII or ChgB (left panel), or overlap of endogenous SecrgII or ChgB with NPY–pHluorin immunoreactivity (right panel). (D–K) Stimulation-dependent fusion of NPY–pHluorin in DIV3 and DIV4 WT and SNAP-25 KO neurons. (D,E) Frequency distribution of DCV fusion events measured with NPY–pHluorin in WT and S25KO neurons before, during and after stimulation in DIV3 and DIV4 neurons, respectively (DIV3 WT: *n*=7 cells, 26 events; DIV3 S25KO: *n*=5 cells, 12 events; *N*=3 independent experiments; DIV4 WT: *n*=13 cells, 69 events; DIV4 S25KO: *n*=8 cells, 13 events; *N*=4 independent experiments). Blue bars represent stimulation of 16 bursts of 50 APs at 50 Hz; inset, typical Ca^{2+} traces in WT (black) and S25KO (red) neurons measured with Fluo5-AM show similar Ca^{2+} dynamics before, during and after stimulation in both genotypes. Ca^{2+} influx is more robust at DIV4 compared to DIV3, note different scale bars for Ca^{2+} measurements in DIV3 and DIV4 neurons. (F) Mean number of DCV fusion events per cell during stimulation in WT and S25KO neurons (DIV3 WT: *n*=7 cells, 26 events; S25KO: *n*=5 cells, 12 events; *N*=3 independent experiments; ns, not significant, Mann–Whitney *P*=0.9178; DIV 4 WT: *n*=13 cells, 69 events; S25KO: *n*=8 cells, 13 events; *N*=4 independent experiments; Mann–Whitney ***P*=0.013; ns, not significant, *P*=0.342). (G,H) Mean cumulative DCV fusion events during stimulation in DIV3 and DIV4 WT and S25KO neurons. Blue bars represent the stimulation period. (I) Mean total number of DCVs, visualized by de-quenching of NPY–pHluorin upon application of NH_4^+ in S25KO and WT neurons at DIV3 and DIV4 measured in F. (DIV3 WT: *n*=7 cells, 1835 vesicles; DIV3 S25KO: *n*=5 cells, 782 vesicles; *N*=3 independent experiments; Mann–Whitney, *P*=0.559; DIV 4 WT: *n*=13 cells, 3937 vesicles; DIV4 S25KO: *n*=8 cells, 1673 vesicles; *N*=4 independent experiments; ns, not significant, Mann–Whitney *P*=0.152 and *P*=0.146 for DIV3 and DIV4). (J,K) Normalized (norm.) fusion probability measured as the ratio of vesicles fused during stimulation per cell to their total pools in DIV3 and DIV4 WT and S25KO neurons (DIV 3 WT: *n*=7 cells; S25KO: *n*=5 cells; *N*=3 independent experiments; ns, not significant, Mann–Whitney, *P*=0.845; DIV 4 WT: *n*=13 cells; S25KO: *n*=8 cells; *N*=4 independent experiments; ns, not significant, *P*=0.635, Mann–Whitney, ***P*=0.011). Data is plotted as mean±s.e.m. Dots in F,I represent individual neurons.

different from that of those expressing SNAP-25 and of WT neurons (Fig. 3E), as reported previously (Delgado-Martínez et al., 2007). In addition, SNAP-25 KO neurons expressing SNAP-23 showed a higher amplitude and more prolonged increase, or slower decline, in SypHy fluorescence after stimulation than WT and SNAP-25 KO neurons expressing SNAP-25 (Fig. 3F). SypHy fluorescence in SNAP-25 KO neurons expressing SNAP-29 showed a small and gradual increase over time (Fig. 3E,F). Hence, expression of SNAP-25 or SNAP-23 restores SV fusion in SNAP-25 KO neurons while expression of SNAP-29 rescued cell survival but not AP-triggered SV fusion.

SNAP-25 homologs rescue DCV fusion in DIV14 SNAP-25 KO neurons to varying extents

We next tested the capacity of SNAP-25-related proteins to support DCV fusion at DIV14 in the absence of SNAP-25. Lentiviral expression of SNAP-25 in SNAP-25 KO neurons, using a similar approach to that described above, fully rescued DCV fusion capacity with a similar number of fusion events and a fusion probability as that in WT neurons (Fig. 4A,C-D). SNAP-23 or SNAP-29 expression in SNAP-25 KO neurons did rescue DCV fusion capacity, albeit with different efficiencies. DCV fusion was 1.5-fold lower in SNAP-23- and sixfold lower in SNAP-29-rescued neurons compared to rescue with SNAP-25 (SNAP-25, 294.1±68.1 fusion events/cell; SNAP-23, 172.3±53.4 events/cell; SNAP-29, 45.1±19.2 events/cell; mean±s.e.m.; Fig. 4A-C). Total DCV numbers in SNAP-25 KO neurons rescued with SNAP-25, SNAP-23 or SNAP-29 were similar and comparable to those in WT (Fig. 4D). DCV fusion probabilities, expressed as the number of fusion events divided by the total DCV pool per cell, were not significantly different between SNAP-23- and SNAP-25-rescued neurons, and were almost sixfold lower in SNAP-29-rescued neurons (Fig. 4D). The DCV fusion rate (number of fusion events over time) was similar between WT and SNAP-25 KO neurons expressing SNAP-25 (Fig. 4E), while fusion rates in SNAP-25 KO neurons expressing SNAP-23 or SNAP-29 were significantly lower (Fig. 4F,G). In WT and SNAP-25 KO neurons expressing SNAP-25, the majority of DCV fusion events occurred between the first and second bursts of 50 APs, whereas in SNAP-25 KO neurons expressing SNAP-23 and SNAP-29, the majority of fusion events occurred in between the sixth and tenth stimulation bursts (Fig. 4H). Hence, SNAP-25-related genes rescue DCV fusion capacity to different extents when expressed in SNAP-25 KO neurons, and the fusion kinetics are different between expression of SNAP-25 and SNAP-23 or SNAP-29.

SNAP-47 expression in SNAP-25 KO neurons does not rescue cell survival, SV or DCV fusion

To examine our observation that SNAP-47 expression does not rescue cell survival of SNAP-25 KO neurons in more depth, we tested SNAP-47 expression levels in DIV14 WT neurons and in the surviving SNAP-25 KO neurons, also upon lentiviral overexpression of SNAP-47. Endogenous and overexpressed SNAP-47 was readily detected in WT and SNAP-25 KO neuronal lysates, and lentiviral expression led to higher SNAP-47 levels (Fig. 5A). However, despite overexpression of SNAP-47, these neurons showed a similar survival profile to that of SNAP-25 KO neurons – neurons developed normally until DIV2-3, after which degeneration occurred, leading to survival of less than 2% of the neurons at DIV8 (Fig. 5B), as reported previously (Delgado-Martínez et al., 2007; Washbourne et al., 2002), and surviving SNAP-25 KO neurons that overexpressed SNAP-47 showed similar reduced synapse numbers and dendrite morphology to SNAP-25 KO neurons (Fig. S4). Further examination using semi-quantitative immunofluorescence analysis showed robust expression of SNAP-47 in synapses of WT, surviving SNAP-25 KO neurons and SNAP-25 KO neurons overexpressing SNAP-47 (Fig. 5C,D). SNAP-47 expression levels were similar in WT and SNAP-25 KO neurons, and lentiviral expression increased SNAP-47 levels approximately threefold in synapses (Fig. 5C-E). Hence, despite high cellular expression levels, SNAP-47 did not rescue survival in SNAP-25 KO neurons.

We next tested if these neurons support SV fusion. To this end, we infected WT, surviving SNAP-25 KO neurons and SNAP-25 KO neurons overexpressing SNAP-25 or SNAP-47 with SypHy. Stimulation with 200 APs at 10 Hz triggered SV fusion in WT and SNAP-25 KO neurons expressing SNAP-25, as expected. However, SV fusion was absent in SNAP-25 KO neurons that overexpressed SNAP-47 – i.e. similar to SNAP-25 KO neurons (Fig. 5F). Also, SNAP-47 overexpression did not increase DCV fusion in SNAP-25 KO neurons, and DCV fusion was still >95% reduced when compared to that of WT and SNAP-25 KO neurons expressing SNAP-25 (Fig. 5G,H). Hence, in contrast to SNAP-23 and SNAP-29, SNAP-47 does not rescue survival of SNAP-25 KO neurons and does not support SV or DCV fusion in the absence of SNAP-25.

Journal of Cell Science (2017) 130, 1877-1889 doi:10.1242/jcs.201889

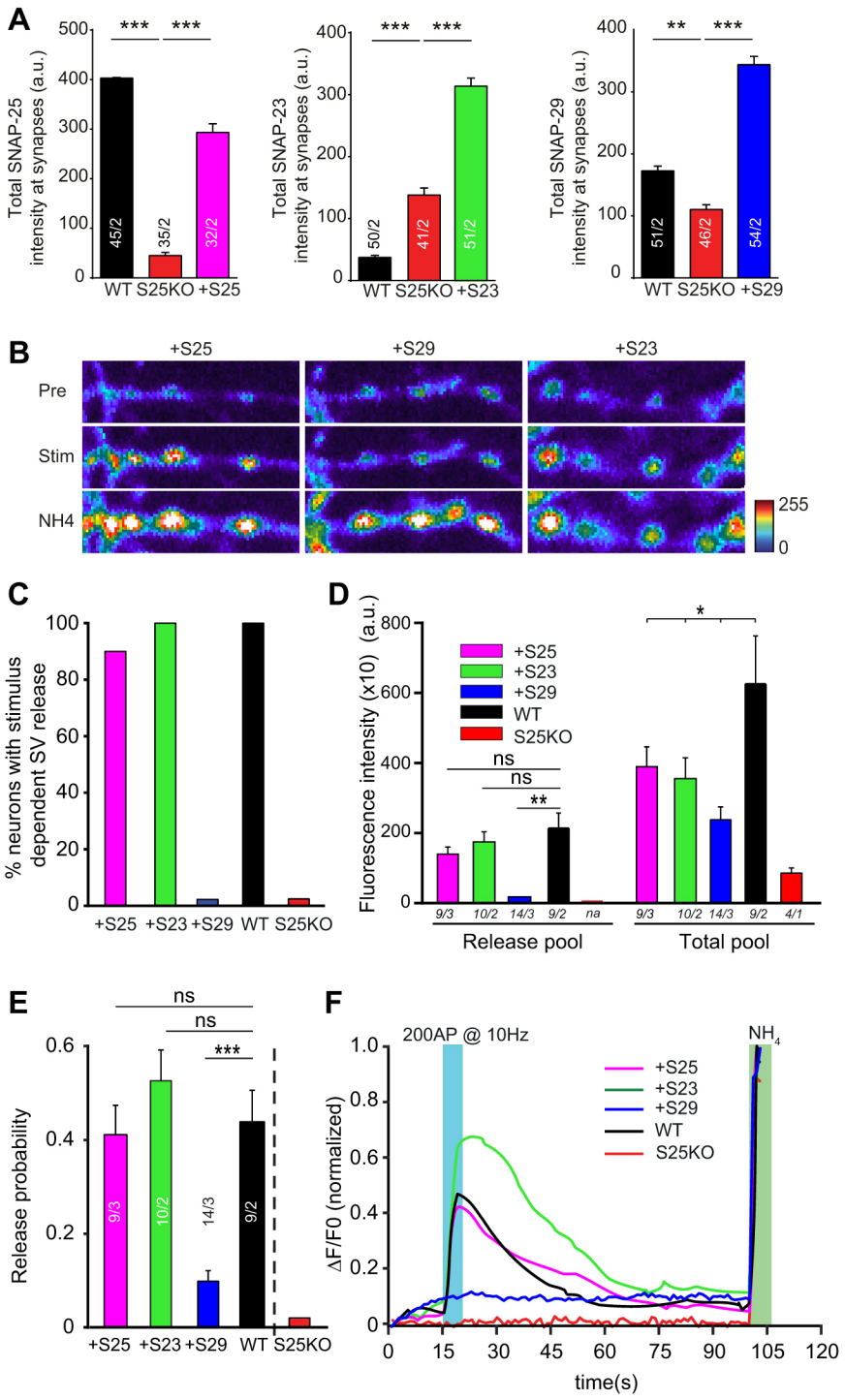

Fig. 3. SNAP-25 family members rescue SV fusion in SNAP-25 KO neurons at DIV14 to varying extents. (A) Mean synaptic intensity of endogenous SNAP-25, SNAP-23 and SNAP-29 and in WT, and surviving SNAP-25 KO (S25KO) neurons and of exogenous SNAP-25, SNAP-23 and SNAP-29 in S25KO neurons upon lentiviral-mediated overexpression (+S25, +S23 or +S29, respectively). Comparisons to KO were significantly different with statistical values of ***P<0.01 or **P=0.013, Dunn's multiple comparisons test. The number of cells and independent experiments are depicted on the bars (separated by a solidus). (B) Typical examples of SypHy fluorescence pre-stimulation (pre), during stimulation (stim) and during NH_4^+ (NH4) application for DIV14 SNAP-25 KO neurons expressing SNAP-25 (+S25), SNAP-29 (+S29) or SNAP-23 (+S23). (C) Percentage of neurons from WT, S25KO and S25KO neurons expressing SNAP homologs that show stimulus-dependent SV fusion. (D) Maximum SypHy fluorescence intensity upon stimulation with 200 AP at 10 Hz (Release pool) and upon NH_4^+ superfusion (Total pool) in WT, S25KO and S25KO neurons expressing SNAP homologs. The number of cells and independent experiments are depicted under the x-axis (separated by a solidus). *P=0.02, **P=0.008; ns, not significant (Mann–Whitney test). (E) Fusion probability expressed as a ratio of fused to total vesicle pool in WT, S25KO and S25KO neurons expressing SNAP homologs. Mann–Whitney, WT versus S29, ***P=0.001. ns, not significant. (F) Normalized ΔF/F0 SypHy fluorescence profiles upon stimulation with 200 AP at 10 Hz (blue bar) in WT, S25KO and S25KO neurons expressing SNAP homologs normalized to the total pool (NH_4^+, green bar). Data are mean±s.e.m.

DISCUSSION

In this study, we show that DCV exocytosis during early development *in vitro* (DIV3) is Ca^{2+} dependent and becomes SNAP-25 dependent at DIV4, before the onset of massive cell death of SNAP-25 KO neurons. Expression of SNAP-25 family members in SNAP-25 KO neurons rescued neuronal survival, DCV and SV fusion to different extents – SNAP-23 supported efficient SV and DCV fusion in the absence of SNAP-25, while expression of SNAP-29 rescued neuronal viability and DCV fusion but not SV fusion. SNAP-47 failed to rescue viability of SNAP-25 KO neurons, and neither supported DCV nor SV fusion in the surviving SNAP-25 KO neurons.

We used the DCV cargo protein NPY coupled to pHluorin to assess activity-dependent fusion of DCVs before synapse formation in developing (DIV3-4) and mature (DIV14) neurons. NPY–pHluorin puncta showed strong colocalization with the endogenous DCV markers secretogranin II and chromogranin B (Fig. 2). Hence, the DCV cargo reporter NPY–pHluorin is properly sorted to secretogranin-II- and chromogranin-B-positive DCVs both in developing and mature neurons. The fact that DCV fusion is virtually abolished in the absence of SNAP-25 indicates that sorting of this reporter to the regulated secretory pathway, as opposed to constitutive secretion, is almost perfect.

Journal of Cell Science (2017) 130, 1877-1889 doi:10.1242/jcs.201889

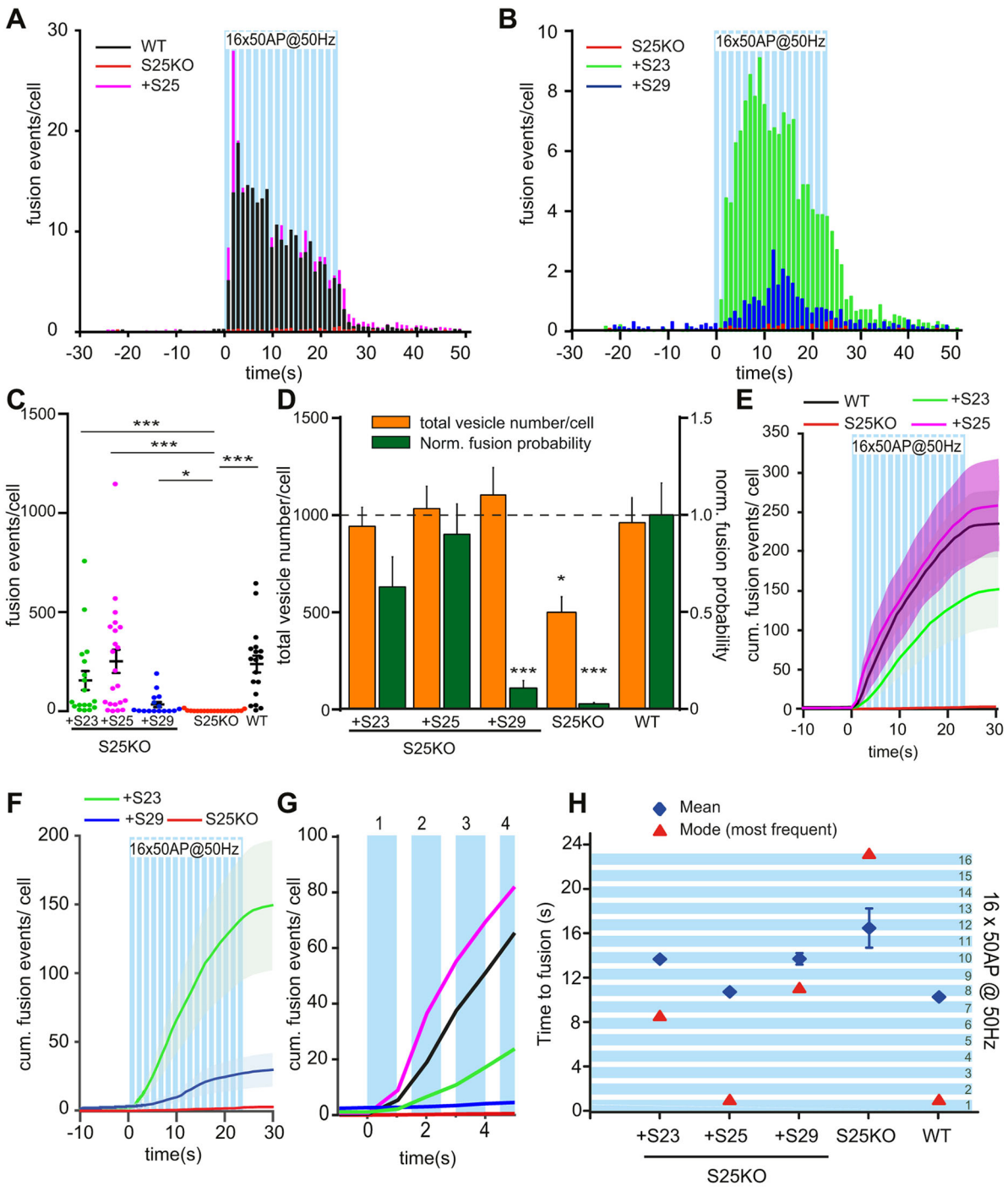

Fig. 4. SNAP-25 family members differentially rescue DCV fusion in SNAP-25 KO neurons at DIV14. (A) Frequency distribution of DCV fusion events from WT, S25KO and S25KO neurons expressing SNAP-25 (+S25). Blue bars represent 16 bursts of 50 APs at 50 Hz. (B) Frequency distribution of DCV fusion events from SNAP-25 KO (S25KO) and S25KO neurons expressing SNAP-23 (+S23) or SNAP-29 (+S29). (C) Mean number of DCV fusion events in WT, S25KO and S25KO neurons expressing SNAP homologs (+S23: *n*=18 cells, *N*=4, 2791 events; +S25: *n*=22 cells, *N*=4, 5538 events; +S29: *n*=16 cells, *N*=4, 541 events; S25KO: *n*=19 cells, *N*=3, 44 events; WT: *n*=18 cells, *N*=4, 4286 events. Mann–Whitney test to compare to KO levels vs S23, ***P<0.001; vs S25, ***P<0.001; vs S29, *P=0.0123; vs WT, ***P<0.001). Dots represent individual cells. (D) Total pool and normalized (norm.) fusion probability (NFP; measured as the ratio of vesicles fused per cell to their total pools) in WT, S25KO and S25KO neurons expressing SNAP homologs (+S23: *n*=15 cells, *N*=4, 14146 vesicles, NFP=0.63; +S25: *n*=21 cells, *N*=4, 21714 vesicles, NFP=0.90; +S29: *n*=15 cells, *N*=4, 16567 vesicles, NFP=0.11; S25KO: *n*=12 cells, *N*=3, 6009 vesicles, NFP=0.03; WT: *n*=18 cells, *N*=4, 17321 vesicles, NFP=1.00). Total vesicle pool KO versus WT, *P=0.024; NFP of KO versus WT, ***P<0.001; NFP of S29 vs WT, ***P<0.001. (E) Mean cumulative (cum.) DCV fusion events before, during and after stimulation in S25KO and S25KO neurons expressing SNAP-25 (+S25) or SNAP-23 (+S23). (F) Mean cumulative DCV fusion events before, during and after stimulation in S25KO and S25KO neurons expressing SNAP-23 (+S23, same trace as in E) or SNAP-29 (+S29). (G) Mean cumulative frequency during the first four bursts of 50 APs at 50 Hz. (H) Mean and mode (most frequent) time of fusion upon AP stimulation in S25KO, WT and S25KO expressing SNAP-25, SNAP-23 or SNAP-29 neurons. Horizontal blue bars represent 50 AP bursts of a 16×50 APs at 50 Hz stimulus train (mean time of fusion: +S23: 43.68±0.21 s, mode: 38.5 s; +S25: 40.76±0.12 s, mode: 31 s; +S29: 43.71±0.51 s, mode: 41 s; S25KO: 46.45±1.75 s, mode: 53 s; WT: 40.30±0.11 s, mode: 31 s). Data are mean±s.e.m.

Journal of Cell Science (2017) 130, 1877-1889 doi:10.1242/jcs.201889

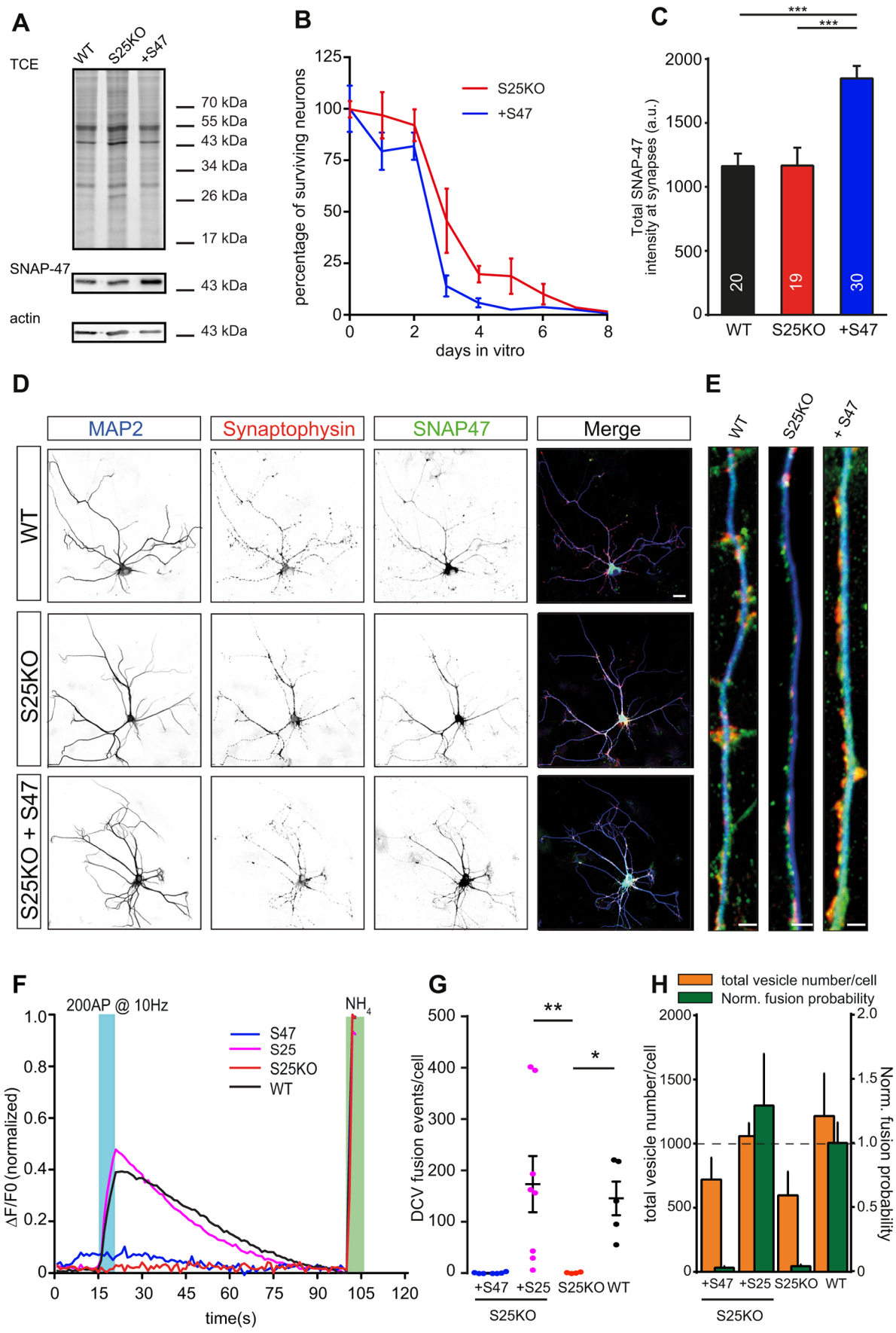

Fig. 5. See next page for legend.

Journal of Cell Science (2017) 130, 1877-1889 doi:10.1242/jcs.201889

Fig. 5. SNAP-47 does not rescue survival, synaptic transmission or DCV fusion in SNAP-25 KO neurons at DIV14. (A) Representative western blot of cultured WT, surviving SNAP-25 KO (S25KO) neurons and S25KO neurons overexpressing SNAP-47 (+S47) stained for SNAP-47 and actin as loading control. Note the overexpression of SNAP-47 in lane 3. TCE, 2,2,2-Trichloroethanol incorporated into gels to assess protein loading. (B) Survival curve comparing the percentage of surviving S25KO neurons and S25KO neurons overexpressing SNAP-47 (+47) from the day of plating (DIV0). SNAP-47 fails to rescue survival of SNAP-25 KO neurons. (C) Mean overall intensity of SNAP-47 at synapses of WT, surviving S25KO neurons and S25KO neurons expressing SNAP-47 (+S47). Mann–Whitney, ***P<0.001. n values are shown on the bars. (D) Representative images of WT, surviving S25KO neurons and S25KO neurons overexpressing SNAP-47 that had been stained for dendrites (MAP2, blue), synapses (synaptophysin, red) and SNAP-47 (green). Scale bar: 10 µm. (E) Zoomed images of regions in D. Scale bars: 3 µm. (F) SypHy responses to 200 APs at 10 Hz in WT, surviving S25KO neurons and S25 KO neurons overexpressing SNAP-25 or SNAP-47 normalized to the total pool upon NH_4^+ superfusion. (G) Mean DCV fusion events in WT, surviving S25KO neurons and S25KO neurons overexpressing SNAP-25 or SNAP-47. (+S47: n=8 cells, N=2, 7 events; +S25: n=8 cells, N=2, 1392 events; S25KO: n=4 cells, N=2, 6 events; WT: n=5 cells, N=2, 732 events; *P=0. 0159, **P=0.004). Dots represent individual neurons. (H) Total pool (orange bars) and normalized fusion probability (green bars, NFP; ratio of vesicles fused per cell to their total pools) in WT, S25KO and S25KO neurons expressing SNAP isoforms (+S47: n=2 cells, N=2, 1441 vesicles, NFP=0.03; +S25: n=6 cells, N=2, 6354 vesicles, NFP=1.29; S25KO: n=3 cells, N=2, 1792 vesicles, NFP=0.04; WT: n=3 cells, N=2, 3646 vesicles, NFP=1.00).

SNAP-25 regulates neuronal morphology and viability

DCV fusion became SNAP-25 dependent at DIV4 prior to the massive cell loss in SNAP-25 KO neurons (Fig. S1; Delgado-Martínez et al., 2007; Washbourne et al., 2002). DCV fusion in the remaining ∼2% of SNAP-25 KO neurons at DIV14 was strongly reduced compared to in WT neurons. Both at DIV4 and DIV14, SNAP-25 KO neurons were smaller, with reduced neurite arborization and, at DIV14, fewer synaptic connections. This suggests that a lack of trophic support, due to impaired DCV fusion, might limit survival of SNAP-25 KO neurons and affect cell morphology in the surviving neurons. However, additional cell intrinsic mechanisms are also likely to play a role given that SNAP-25 KO neurons showed reduced dendrite length as early as DIV3, when DCV fusion was unaffected by SNAP-25 deletion (Fig. S2), and that and other models in which DCV fusion is blocked, such as in VAMP2 KO neurons and WT neurons treated with Tetanus toxin (which cleaves VAMP1, VAMP2 and VAMP3), do not degenerate (Peng et al., 2013; Schoch et al., 2001).

SNAP-25 is the major SNAP homolog for DCV fusion in DIV14 hippocampal neurons

DCV fusion in SNAP-25 KO neurons at 14 DIV was almost abolished (Fig. 1). These findings are in line with previous studies demonstrating reduced BDNF release in hippocampal neurons upon shRNA-mediated knockdown of SNAP-25 (Shimojo et al., 2015) and secretory granule release in SNAP-25 KO chromaffin cells (Sørensen et al., 2003). As SNAP-25 deletion also blocks SV fusion (Delgado-Martínez et al., 2007; Washbourne et al., 2002), these findings show that SNAP-25-dependent SNARE machinery drives fusion of the two major secretory pathways in parallel, and that endogenous expression of other SNAP-25 protein family members is insufficient to support secretion in the absence of SNAP-25. Viral expression of SNAP-23, the closest homolog of SNAP-25, in SNAP-25 KO neurons rescued cell survival and Ca^{2+}-dependent SV and DCV fusion almost as efficiently as expression of SNAP-25 in SNAP-25 KO neurons (Figs 3 and 4). This shows that, in principle, SNAP-23 is able to replace SNAP-25 in a SNARE complex that couples Ca^{2+} influx to vesicle fusion. However, DCV fusion in SNAP-25 KO neurons that had been rescued with SNAP-23 required prolonged stimulation and did not fully reach WT levels (Fig. 4E-H). In addition, SV fusion was more asynchronous to the 200 APs at 10 Hz stimulation (Fig. 3F). This can be explained by the fact that, in contrast to SNAP-25, SNAP-23 does not bind to synaptotagmin-1, the Ca^{2+} sensor for fast synchronous fusion, but instead binds to synaptotagmin-7 (Chieregatti et al., 2004), implicated in exocytosis in neuroendocrine cells (Schonn et al., 2008; Sugita et al., 2001) and asynchronous SV fusion in neurons (Bacaj et al., 2013; Weber et al., 2014). Delayed vesicle fusion upon Ca^{2+} entry of synaptotagmin-7-labeled secretory granules compared to synaptotagmin-1-labeled vesicles has also been observed in adrenal chromaffin cells (Rao et al., 2014). In these cells, synaptotagmin-1 and synaptotagmin-7 appear to label different secretory granule populations. Although we cannot rule out the existence of different DCV pools in neurons, the finding that in the absence of SNAP-25, evoked DCV fusion is largely abolished does not support a major role for SNAP-23–synaptotagmin-7 complexes in driving Ca^{2+}-dependent DCV fusion in SNAP-25 KO neurons at DIV14. However, a SNAP-23–synaptotagmin-7 complex may be involved in DCV fusion during early development before the developmental switch to SNAP-25-dependent fusion (see below).

SNAP-29 rescues neuronal viability and DCV but not SV fusion

Like SNAP-23, SNAP-29 rescued the lethal phenotype of SNAP-25 KO neurons and completely restored total DCV numbers in SNAP-25 KO neurons. It also supported DCV fusion, albeit much less efficiently compared to SNAP-25- or SNAP-23-rescued neurons, but not SV fusion. As SNAP-29, in contrast to SNAP-25 and SNAP-23, lacks the cysteine domains that are palmitoylated in SNAP-25 and SNAP-23 (Steegmaier et al., 1998), this indicates that to support neuronal survival, DCV biogenesis and, to a lesser extent, DCV fusion, protein palmitoylation is not required. It also suggests that SNAP-29 is able to engage in a plasma-membrane–SNARE complex via a palmitoylation-independent process to support DCV fusion but that such a complex cannot support SV fusion.

SNAP-29 functions in constitutive release in non-neuronal cells, interacting with syntaxin-19 (Gordon et al., 2010), and in intracellular fusion of autophagosomes with endo-lysosomes in a SNARE complex with syntaxin-17 (Itakura et al., 2012), but SNAP-29 also interacts with other plasma membrane syntaxins (Steegmaier et al., 1998) and has recently been implicated in secretory autophagy in combination with syntaxin-3 and syntaxin-4 (Kimura et al., 2017). Overexpressed SNAP-29 does not efficiently replace SNAP-25 in the SNARE-complex-driving SV fusion (Fig. 3). This is in line with previous findings that SNAP-29 inhibits SV fusion when overexpressed in a WT background, probably by hindering canonical SNARE complex disassembly and synaptic vesicle turnover (Pan et al., 2005; Su et al., 2001). Our results show that in neurons, SNAP-29 is able to support regulated release of DCV cargo to some extent (Fig. 4) but not SV fusion, which indicates that an alternative SNARE complex supports SNAP-29-dependent DCV fusion in the absence of SNAP-25, albeit much less efficiently than SNAP-25. The incomplete restoration of DCV fusion may also explain why expression of SNAP-29 does not rescue all morphological defects of SNAP-25 KO neurons (Fig. S3N-R).

Journal of Cell Science (2017) 130, 1877-1889 doi:10.1242/jcs.201889

SNAP-47 does not rescue neuronal viability, nor does it support DCV or SV fusion, suggesting a function upstream of SNAP-25

In contrast to SNAP-23, and SNAP-29, SNAP-47 did not rescue cell viability of SNAP-25 KO neurons (Fig. 5), nor did it support SV and DCV fusion in the surviving SNAP-25 KO neurons (Fig. 5). Although initially discovered in subcellular fractionation studies in the fraction enriched in small synaptic vesicles (Holt et al., 2006), SNAP-47 appears to have a widespread intracellular localization – in neurons, SNAP-47 is present in cytosol and neurites but, in contrast to SNAP-25 and SNAP-23, is not selectively localized to the plasma membrane or to presynaptic nerve terminals (Fig. 5D,E; Holt et al., 2006). In Hela cells, SNAP-47 localizes to the endoplasmic reticulum (ER) and ER-Golgi intermediate compartment (ERGIC) where it interacts with VAMP4, VAMP7 and VAMP8 (Kuster et al., 2015). SNAP-47 can substitute for SNAP-25 in a complex of syntaxin1 and VAMP2 in SNARE-driven fusion of liposomes, but it does so with strongly reduced efficiency (Holt et al., 2006) and it only weakly interacts with VAMP2, the VAMP isoform involved in SV and DCV fusion (Kuster et al., 2015). However, shRNA-mediated depletion of SNAP-47 blocks axonal release of brain-derived neurotrophic factor (BDNF) in neurons (Shimojo et al., 2015) and also affects fusion of AMPA-receptor-containing organelles (Arendt et al., 2015; Jurado et al., 2013). Hence, these observations suggest a role for SNAP-47 in fusion of neurotrophic factor vesicles (DCVs) and AMPA-receptor vesicles with the plasma membrane. In contrast, our data show that for DCV and SV fusion, SNAP-47 cannot execute this role in the absence of SNAP-25. Hence, based on its subcellular localization, the interaction with ER-resident VAMP isoforms in heterologous cells and the lack of synaptic enrichment, it is conceivable that SNAP-47 functions upstream of SNAP-25 in the secretory pathway, possibly contributing to proper subcellular localization and function of VAMP4, VAMP7 and VAMP8, rather than at the plasma membrane controlling fusion of secretory vesicles. As SNAP-47-dependent BDNF release has been tested in the presence of SNAP-25 (Shimojo et al., 2015), it is plausible that both proteins function in a similar pathway and that efficient BDNF release requires the orchestrated action of both SNAP isoforms, with SNAP-47 most likely acting upstream of SNAP-25.

During early development, NPY–pHluorin fusion events were already highly synchronous to the Ca^{2+} influx (Fig. 2), suggesting that a regulated secretory pathway, most likely exploiting SNAREs and Ca^{2+} sensors, becomes operational at an early developmental phase. Neurons gradually acquire this capacity during the first days *in vitro* as the number of cells unresponsive to Ca^{2+} stimulation reduced from ∼60% at DIV3 to ∼40% at DIV4 and ∼5% at DIV14 (Fig. 2). It has been proposed that before synapse formation, specialized vesicles, referred to as piccolo–bassoon transport vesicles (PTVs), ship active zone components to nascent synapses. Like the DCVs studied here, PTVs also have a dense core and are chromogranin B positive (Zhai et al., 2001). Based on the high colocalization of NPY–pHluorin with chromogranin B and secretogranin II at DIV4, we conclude that NPY–pHluorin also labels PTVs, which may suggest that PTVs can be delivered to the membrane in an activity-dependent manner from DIV3-4 onwards. Such a mechanism may operate to supply nascent active synapses with additional presynaptic release machinery components to increase efficient synaptic transmission.

Our data (Fig. 2) show that Ca^{2+}-dependent DCV fusion before DIV4 appears to be regulated by a SNAP-25-independent mechanism (Fig. 2). Based on the expression profiles of SNAP homologs and their capacity to support DCV fusion, the most plausible SNAP to operate at this early time point is SNAP-23. SNAP-23 is expressed during early brain development (Prescott and Chamberlain, 2011; Suh et al., 2010) and its deletion leads to embryonic lethality during early embryo development (Suh et al., 2011). SNAP-25 expression levels are initially low but strongly increase during late pre- and early postnatal development (Prescott and Chamberlain, 2011; Suh et al., 2010). Also in our culture system, SNAP-23 levels are significantly higher at DIV3 than at DIV4 in WT and SNAP-25 KO neurons (Fig. S2J-L). Hence, it is conceivable that before DIV4, DCV fusion is regulated by a SNAP-23-dependent SNARE complex, which is gradually replaced by the canonical SNAP-25-dependent complex from DIV4 onwards. In adrenal chromaffin cells, SNAP-23–synaptotagmin-7 SNARE complexes drive efficient secretory granule exocytosis upon mild stimuli, which lead to a moderate elevation of intracellular Ca^{2+} levels (Rao et al., 2014). Hence, before efficient clustering of Ca^{2+} channels in presynaptic compartments, a SNAP-23-dependent SNARE complex may operate more efficiently to fuse DCVs in developing neurons. When synapses become functional, SNAP-25-dependent fusion machinery, with stricter coupling between Ca^{2+} influx and DCV fusion (Fig. 4H), would then ensure properly timed Ca^{2+}-dependent fusion of DCVs.

In conclusion, we have shown that SNAP-25 is the canonical SNAP homolog to drive efficient DCV fusion in neurons, suggesting that DCV and SV fusion is governed by similar SNARE machinery in mature neurons. Different SNARE complexes and Ca^{2+} sensors may be able to replace each other for DCV fusion, but less so for SV fusion. Finally, we have identified a developmental switch, in cultured hippocampal neurons between DIV3 and DIV4, through which evoked DCV fusion becomes SNAP-25 dependent.

MATERIALS AND METHODS

Laboratory animals

Embryonic day (E)18 SNAP-25 KO embryos were obtained by cesarean section of time-mated SNAP-25 heterozygous mice (Washbourne et al., 2002). WT littermates were used as controls. All animal experiments were performed in compliance with the guidelines for welfare of experimental animals issued by the Dutch government and approved by the ethical committee of the Vrije Universiteit, Amsterdam.

Primary neuronal culture

Single neuron suspensions were prepared from hippocampi of E18 mice according to de Wit et al. (2009). Continental cultures with 25,000 neurons/well (WT) or 300,000 neurons/well (SNAP-25 KO) were plated on pre-made cultures of rat glia cells (37,500 cells/well) on 18-mm glass coverslips in 12-well plates and cultured in Neurobasal medium (Invitrogen) supplemented with 2% B-27 (Invitrogen), 1.8% HEPES, 1% Glutamax (Gibco, UK) and 1% penicillin-streptomycin (Invitrogen). For single isolated neuronal island cultures as described previously (Toonen et al., 2006; Wierda et al., 2007), neurons were plated at a density of 1400 (WT) or 8000 neurons/well (SNAP-25 KO) on 18-mm glass coverslips in 12-well plates on rat glia micro-islands. Rat glia micro-islands were prepared by plating 8000 glia cells/well on 18-mm glass coverslips coated with agarose and stamped with a solution comprising 0.1 mg/ml poly-D-lysine (Sigma) and 0.2 mg/ml rat tail collagen (BD Biosciences). Neuron survival curves were generated by plating 300,000 WT or SNAP-25 KO neurons, or SNAP-25 KO neurons expressing the different SNAP isoforms, without glia. Neurons were manually counted at each DIV. Graphs were normalized to density at plating (DIV 0).

Plasmids and lentiviral infection

NPY–pHluorin and synapsin1–mCherry have been previously described (Farina et al., 2015; van de Bospoort et al., 2012). Synapsin–ECFP was

generated by replacing mCherry with ECFP. SypHy has been described previously (Granseth et al., 2006). cDNAs for mouse SNAP-25, SNAP-23, SNAP-29 and SNAP-47 were generated from a mouse brain cDNA library (Invitrogen) using standard PCR techniques and sequence verified. SNAP-25 isoform b was used for all rescue experiments. cDNAs were cloned into lentiviral vectors (as described previously, Farina et al., 2015; van de Bospoort et al., 2012) under the control of a human synapsin promoter that co-expressed nucleus-targeted mCherry (Cre-mCherry) using an IRES sequence. Lentiviral production was performed as described previously (Farina et al., 2015; van de Bospoort et al., 2012). SypHy and Synapsin–ECFP infections were performed at DIV7, and neurons were imaged between DIV14 and DIV18. NPY–pHluorin infections were performed at DIV10 for neurons imaged between DIV14 and DIV18, and on DIV0 for neurons imaged at DIV3 and DIV4. SNAP-25 KO neurons were rescued with SNAP-23, SNAP-25, SNAP-29 or SNAP-47 Cre-mCherry constructs on DIV1, as described previously (Delgado-Martínez et al., 2007). Rescued neurons were subsequently infected with NPY–pHluorin as stated above and imaged between DIV14 and DIV18.

Imaging

maging was performed on an inverted fluorescence microscope (lX81; Olympus) equipped with a MT20 light source (Olympus), appropriate filter sets (Semrock, Rochester, NY), 40× oil objective (NA 1.3) and an electron multiplying charge-coupled device (C9100-02; Hamamatsu Photonics, Japan) driven by Xcellence RT imaging software (Olympus). Coverslips were placed in an imaging chamber and perfused with Tyrode's buffer (2 mM $CaCl_2$, 2.5 mM KCl, 119 mM NaCl, 2 mM $MgCl_2$, 20 mM glucose, 25 mM HEPES, pH 7.4). During SypHy and NPY–pHluorin experiments, intracellular pH was neutralized with Tyrode's solution, in which 50 mM NaCl was replaced by 50 mM NH_4Cl, applied by gravity flow through a glass capillary placed between two platinum electrodes that were used to deliver 30 mA 1 ms electrical stimulations via a stimulus generator (A385RC, World Precision Instruments, Germany). The stimulus used for DCV fusion comprised 16 trains of 50 APs at 50 Hz with 500 ms intervals, as described previously (de Wit et al., 2009; van de Bospoort et al., 2012). The stimulus used for SypHy measurements was 200 APs at 10 Hz. Experiments were performed at room temperature (21-24°C). Data for DCV and synaptophysin assays were acquired at sampling rates of 2 Hz and 1 Hz, respectively. Synapsin masks and Cre–mCherry signals were acquired at 1 Hz before stimulating neurons for DCV assays.

Image analysis

Time-lapse images of DCV fusion were analyzed by selecting a 3×3 pixel region (0.45 µm×0.45 µm). Differences between fluorescence changes were expressed as ΔF and compared to baseline fluorescence (F0), which was the mean value of the first four frames. A DCV fusion event was detected as a sudden rise in fluorescence at least twofold above baseline. Fusion events were scored as synaptic when the fluorescence center of a release event was within 200 nm (±1 pixel) of the synapsin–ECFP fluorescence centroid. We only measured fusion events from neurites and excluded somatic fusion events as these cannot be reliably measured using wide-field fluorescence microscopy due to the bright fluorescence from vesicles in or near the Golgi in which the intraluminal pH is not yet acidic. The total number of vesicles was manually analyzed by counting fluorescent DCV puncta from the frames acquired upon NH_4^+ application.

Time-lapse images of SypHy assays were analyzed by selecting a 3×3 pixel region (0.45 µm×0.45 µm). Differences between fluorescence changes were expressed as ΔF and compared to the baseline fluorescence (F0), which was the mean of the first five frames. ΔFmax (total vesicle pool) was calculated as the highest ΔF value during NH_4^+ application. ΔF/ΔFmax indicates the total fusion pool.

Analysis of confocal images was performed with SynD software (Schmitz et al., 2011) using default settings. The ratio of glutamatergic versus GABAergic neurons was assessed by immunofluorescence labeling of DIV14 WT or SNAP-25 KO neurons with antibodies against VGLUT1 and VGAT, and manual counting of 20 fields of view of three independent cultures using a 40× objective. Colocalization (Manders' and Pearson's) of NPY–pHluorin and endogenous DCV cargo was analyzed with ImageJ plugin JACoP using default settings. NPY–pHluorin signal was amplified using EGFP antibody (mouse monoclonal, Clontech, 632569).

Statistics

Shapiro and Levene's tests were used to assess distribution normality and homogeneity of variances, respectively. When assumptions of normality or homogeneity of variances were met, parametric tests were used: Student's *t*-test or one-way ANOVA (Tukey as post-hoc test). Otherwise, non-parametric tests were used: Mann–Whitney or Kruskal–Wallis with Dunn's correction. Data plotted represent mean±s.e.m. *n* indicates the number of neurons and *N* is the number of independent experiments.

Immunocytochemistry and confocal imaging

Neurons were fixed in 4% formaldehyde (Electron Microscopies Sciences, Germany) in PBS (Gibco), pH 7.4, for 20 min at room temperature. Cells were permeabilized for 5 min in PBS containing 0.5% Triton X-100 (Sigma-Aldrich) and incubated for 30 min with PBS containing 2% normal goat serum and 0.1% Triton X-100. Incubations with primary antibodies and secondary antibodies were performed for 1.5 h and 1 h, respectively, at room temperature. Primary antibodies used were: polyclonal against MAP2 (Abcam, ab5392; 1:500), polyclonal against chromogranin B (SySy, Germany, 259103; 1:500), polyclonal against synaptophysin (SySy, Germany, 101004; 1:250), polyclonal against VGLUT1 (Millipore, AB5905; 1:5000), polyclonal against secretogranin II (Biodesign International, K55101R; 1:500), monoclonal against smi312 (Biolegend, 837901; 1:1000), monoclonal against SNAP-25 (Sternberger, SMI-81; 1:1000), polyclonal against SNAP-23 (SySy, Germany, 111202; 1:50), polyclonal against SNAP-29 (SySy, Germany, 111303; 1:500) and polyclonal against SNAP-47 (SySy, Germany, 111403; 1:500). Alexa-Fluor-conjugated secondary antibodies were purchased from Invitrogen. Coverslips were mounted in Mowiol and examined on a Zeiss LSM 510 confocal microscope with a 40× (NA 1.3) or 60× objectives (NA 1.4).

Western blot analysis

To characterize protein expression levels of SNAP isoforms, cultured SNAP-25 KO and WT cortical neurons uninfected or expressing SNAP isoforms were washed in PBS at DIV14 and homogenized in Laemmli sample buffer comprising 2% SDS, 10% glycerol, 0.26 M β-mercaptoethanol, 60 mM Tris-HCl, pH 6.8, and 0.01% Bromophenol Blue. E18 brain lysates were made by grinding brain tissue in PBS. After spinning down, pellets were resuspended in Laemmli sample buffer (weight to volume: 0.01 g in 0.1 ml). Samples were separated on 12% SDS-polyacrylamide gels and transferred to PVDF membranes using standard techniques. Blots were incubated in 2% milk and 0.5% bovine serum albumin (BSA) in PBS containing 0.1% Tween-20 (PBS Tween) for 1 h at 4°C, and incubated with primary antibodies: monoclonal against SNAP-25 (Sternberger, SMI-81; 1:500), polyclonal against SNAP-23 (SySy, Germany, 111202; 1:500), polyclonal against SNAP-29 (SySy, Germany, 111303; 1:500), polyclonal against SNAP-47 (SySy, Germany, 111403; 1:500) and against actin (Chemicon, MAB1501; 1:2000) in PBS-Tween for 16 h at 4°C. After washing, blots were incubated with anti-rabbit or anti-mouse secondary antibodies (Jackson ImmunoResearch Laboratories company) in PBS Tween for 1 h at room temperature. Blots were scanned using a Fuji Film FLA 5000. Results were analyzed using GelAnalyzer plugin in ImageJ (National Institutes of Health, Bethesda, MD).

Acknowledgements

The authors thank Robbert Zalm for cloning and producing viral particles, Frank den Oudsten and Desiree Schut for producing glia feeders, and Joost Hoetjes for genotyping.

Competing interests

The authors declare no competing or financial interests.

Author contributions

Conceptualization: S.A., M.V., R.T.; Methodology: S.A.; Validation: I.S.; Formal analysis: S.A., R.K., R.v.d.B.; Data curation: S.A., I.S., R.K., R.v.d.B.; Writing - original draft: S.A., R.T.; Writing - review & editing: S.A., M.V., R.T.; Supervision: R.T.; Funding acquisition: M.V.

Funding
This work is supported by a European Research Council Advanced Grant (322966) of the European Union (to M.V.).

Supplementary information
Supplementary information available online at
http://jcs.biologists.org/lookup/doi/10.1242/jcs.201889.supplemental

References

Arendt, K. L., Zhang, Y., Jurado, S., Malenka, R. C., Südhof, T. C. and Chen, L. (2015). Retinoic acid and LTP recruit postsynaptic AMPA receptors using distinct SNARE-dependent mechanisms. *Neuron* **86**, 442-456.
Bacaj, T., Wu, D., Yang, X., Morishita, W., Zhou, P., Xu, W., Malenka, R. C. and Südhof, T. C. (2013). Synaptotagmin-1 and synaptotagmin-7 trigger synchronous and asynchronous phases of neurotransmitter release. *Neuron* **80**, 947-959.
Balkowiec, A. and Katz, D. M. (2002). Cellular mechanisms regulating activity-dependent release of native brain-derived neurotrophic factor from hippocampal neurons. *J. Neurosci.* **22**, 10399-10407.
Bartfai, T., Iverfeldt, K., Fisone, G. and Serfozo, P. (1988). Regulation of the release of coexisting neurotransmitters. *Annu. Rev. Pharmacol. Toxicol.* **28**, 285-310.
Bartolomucci, A., Possenti, R., Mahata, S. K., Fischer-Colbrie, R., Loh, Y. P. and Salton, S. R. J. (2011). The extended granin family: structure, function, and biomedical implications. *Endocr. Rev.* **32**, 755-797.
Chieregatti, E., Chicka, M. C., Chapman, E. R. and Baldini, G. (2004). SNAP-23 functions in docking/fusion of granules at low Ca^{2+}. *Mol. Biol. Cell.* **15**, 1918-1930.
de Wit, J., Toonen, R. F., Verhaagen, J. and Verhage, M. (2006). Vesicular trafficking of semaphorin 3A is activity-dependent and differs between axons and dendrites. *Traffic* **7**, 1060-1077.
de Wit, J., Toonen, R. F. and Verhage, M. (2009). Matrix-dependent local retention of secretory vesicle cargo in cortical neurons. *J. Neurosci.* **29**, 23-37.
Delgado-Martínez, I., Nehring, R. B. and Sørensen, J. B. (2007). Differential abilities of SNAP-25 homologs to support neuronal function. *J. Neurosci.* **27**, 9380-9391.
Farina, M., van de Bospoort, R., He, E., Persoon, C. M., van Weering, J. R. T., Broeke, J. H., Verhage, M. and Toonen, R. F. (2015). CAPS-1 promotes fusion competence of stationary dense-core vesicles in presynaptic terminals of mammalian neurons. *Elife* **4**, e05438.
Ferro-Novick, S. and Jahn, R. (1994). Vesicle fusion from yeast to man. *Nature* **370**, 191-193.
Gordon, D. E., Bond, L. M., Sahlender, D. A. and Peden, A. A. (2010). A targeted siRNA screen to identify SNAREs required for constitutive secretion in mammalian cells. *Traffic* **11**, 1191-1204.
Granseth, B., Odermatt, B., Royle, S. J. and Lagnado, L. (2006). Clathrin-mediated endocytosis is the dominant mechanism of vesicle retrieval at hippocampal synapses. *Neuron* **51**, 773-786.
Hammarlund, M., Watanabe, S., Schuske, K. and Jorgensen, E. M. (2008). CAPS and syntaxin dock dense core vesicles to the plasma membrane in neurons. *J. Cell Biol.* **180**, 483-491.
Hartmann, M., Heumann, R. and Lessmann, V. (2001). Synaptic secretion of BDNF after high-frequency stimulation of glutamatergic synapses. *EMBO J.* **20**, 5887-5897.
Holt, M., Varoqueaux, F., Wiederhold, K., Takamori, S., Urlaub, H., Fasshauer, D. and Jahn, R. (2006). Identification of SNAP-47, a novel Qbc-SNARE with ubiquitous expression. *J. Biol. Chem.* **281**, 17076-17083.
Huang, E. J. and Reichardt, L. F. (2001). Neurotrophins: roles in neuronal development and function. *Annu. Rev. Neurosci.* **24**, 677-736.
Itakura, E., Kishi-Itakura, C. and Mizushima, N. (2012). The hairpin-type tail-anchored SNARE syntaxin 17 targets to autophagosomes for fusion with endosomes/lysosomes. *Cell* **151**, 1256-1269.
Jahn, R. and Fasshauer, D. (2012). Molecular machines governing exocytosis of synaptic vesicles. *Nature* **490**, 201-207.
Jurado, S., Goswami, D., Zhang, Y., Molina, A. J. M., Südhof, T. C. and Malenka, R. C. (2013). LTP requires a unique postsynaptic SNARE fusion machinery. *Neuron* **77**, 542-558.
Kimura, T., Jia, J., Kumar, S., Choi, S. W., Gu, Y., Mudd, M., Dupont, N., Jiang, S., Peters, R., Farzam, F. et al. (2017). Dedicated SNAREs and specialized TRIM cargo receptors mediate secretory autophagy. *EMBO J.* **36**, 42-60.
Kormos, V. and Gaszner, B. (2013). Role of neuropeptides in anxiety, stress, and depression: from animals to humans. *Neuropeptides* **47**, 401-419.
Kuster, A., Nola, S., Dingli, F., Vacca, B., Gauchy, C., Beaujouan, J.-C., Nunez, M., Moncion, T., Loew, D., Formstecher, E. et al. (2015). The Q-soluble N-ethylmaleimide-sensitive factor attachment protein receptor (Q-SNARE) SNAP-47 regulates trafficking of selected Vesicle-associated Membrane Proteins (VAMPs). *J. Biol. Chem.* **290**, 28056-28069.
Ludwig, M. and Leng, G. (2006). Dendritic peptide release and peptide-dependent behaviours. *Nat. Rev. Neurosci.* **7**, 126-136.
Matsuda, N., Lu, H., Fukata, Y., Noritake, J., Gao, H., Mukherjee, S., Nemoto, T., Fukata, M. and Poo, M.-M. (2009). Differential activity-dependent secretion of brain-derived neurotrophic factor from axon and dendrite. *J. Neurosci.* **29**, 14185-14198.
McAllister, A. K., Katz, L. C. and Lo, D. C. (1999). Neurotrophins and synaptic plasticity. *Annu. Rev. Neurosci.* **22**, 295-318.
McMahon, H. T., Foran, P., Dolly, J. O., Verhage, M., Wiegant, V. M. and Nicholls, D. G. (1992). Tetanus toxin and botulinum toxins type A and B inhibit glutamate, gamma-aminobutyric acid, aspartate, and met-enkephalin release from synaptosomes. *Clues to the locus of action*. *J. Biol. Chem.* **267**, 21338-21343.
Meyer-Lindenberg, A., Domes, G., Kirsch, P. and Heinrichs, M. (2011). Oxytocin and vasopressin in the human brain: social neuropeptides for translational medicine. *Nat. Rev. Neurosci.* **12**, 524-538.
Pan, P.-Y., Cai, Q., Lin, L., Lu, P.-H., Duan, S. and Sheng, Z.-H. (2005). SNAP-29-mediated modulation of synaptic transmission in cultured hippocampal neurons. *J. Biol. Chem.* **280**, 25769-25779.
Peng, L., Liu, H., Ruan, H., Tepp, W. H., Stoothoff, W. H., Brown, R. H., Johnson, E. A., Yao, W.-D., Zhang, S.-C. and Dong, M. (2013). Cytotoxicity of botulinum neurotoxins reveals a direct role of syntaxin 1 and SNAP-25 in neuron survival. *Nat. Commun.* **4**, 1472.
Poo, M.-M. (2001). Neurotrophins as synaptic modulators. *Nat. Rev. Neurosci.* **2**, 24-32.
Prescott, G. R. and Chamberlain, L. H. (2011). Regional and developmental brain expression patterns of SNAP25 splice variants. *BMC Neurosci.* **12**, 35.
Rao, T. C., Passmore, D. R., Peleman, A. R., Das, M., Chapman, E. R. and Anantharam, A. (2014). Distinct fusion properties of synaptotagmin-1 and synaptotagmin-7 bearing dense core granules. *Mol. Biol. Cell* **25**, 2416-2427.
Samson, A. L. and Medcalf, R. L. (2015). Tissue-type plasminogen activator: a multifaceted modulator of neurotransmission and synaptic plasticity. *Neuron* **50**, 673-678.
Schmitz, S. K., Hjorth, J. J. J., Joemai, R. M. S., Wijntjes, R., Eijgenraam, S., de Bruijn, P., Georgiou, C., de Jong, A. P. H., van Ooyen, A., Verhage, M. et al. (2011). Automated analysis of neuronal morphology, synapse number and synaptic recruitment. *J. Neurosci. Methods* **195**, 185-193.
Schoch, S., Deak, F., Konigstorfer, A., Mozhayeva, M., Sara, Y., Sudhof, T. C. and Kavalali, E. T. (2001). SNARE function analyzed in synaptobrevin/VAMP knockout mice. *Science* **294**, 1117-1122.
Schonn, J.-S., Maximov, A., Lao, Y., Sudhof, T. C. and Sorensen, J. B. (2008). Synaptotagmin-1 and -7 are functionally overlapping Ca2+ sensors for exocytosis in adrenal chromaffin cells. *Proc. Natl. Acad. Sci. USA* **105**, 3998-4003.
Shimojo, M., Courchet, J., Pieraut, S., Torabi-Rander, N., Sando, R., III, Polleux, F. and Maximov, A. (2015). SNAREs controlling vesicular release of BDNF and development of callosal axons. *Cell Rep.* **11**, 1054-1066.
Sørensen, J. B., Nagy, G., Varoqueaux, F., Nehring, R. B., Brose, N., Wilson, M. C. and Neher, E. (2003). Differential control of the releasable vesicle pools by SNAP-25 splice variants and SNAP-23. *Cell* **114**, 75-86.
Steegmaier, M., Yang, B., Yoo, J. S., Huang, B., Shen, M., Yu, S., Luo, Y. and Scheller, R. H. (1998). Three novel proteins of the syntaxin/SNAP-25 family. *J. Biol. Chem.* **273**, 34171-34179.
Su, Q., Mochida, S., Tian, J.-H., Mehta, R. and Sheng, Z.-H. (2001). SNAP-29: a general SNARE protein that inhibits SNARE disassembly and is implicated in synaptic transmission. *Proc. Natl. Acad. Sci. USA* **98**, 14038-14043.
Südhof, T. C. (2013). Neurotransmitter release: the last millisecond in the life of a synaptic vesicle. *Neuron* **80**, 675-690.
Südhof, T. C. and Rothman, J. E. (2009). Membrane fusion: grappling with SNARE and SM proteins. *Science* **323**, 474-477.
Sugita, S., Han, W., Butz, S., Liu, X., Fernández-Chacón, R., Lao, Y. and Südhof, T. C. (2001). Synaptotagmin VII as a plasma membrane Ca(2+) sensor in exocytosis. *Neuron* **30**, 459-473.
Suh, Y. H., Terashima, A., Petralia, R. S., Wenthold, R. J., Isaac, J. T. R., Roche, K. W. and Roche, P. A. (2010). A neuronal role for SNAP-23 in postsynaptic glutamate receptor trafficking. *Nat. Neurosci.* **13**, 338-343.
Suh, Y. H., Yoshimoto-Furusawa, A., Weih, K. A., Tessarollo, L., Roche, K. W., Mackem, S. and Roche, P. A. (2011). Deletion of SNAP-23 results in pre-implantation embryonic lethality in mice. *PLoS ONE* **6**, e18444.
Takamori, S., Holt, M., Stenius, K., Lemke, E. A., Grønborg, M., Riedel, D., Urlaub, H., Schenck, S., Brügger, B., Ringler, P. et al. (2006). Molecular anatomy of a trafficking organelle. *Cell* **127**, 831-846.
Toonen, R. F. G., Wierda, K., Sons, M. S., de Wit, H., Cornelisse, L. N., Brussaard, A., Plomp, J. J. and Verhage, M. (2006). Munc18-1 expression levels control synapse recovery by regulating readily releasable pool size. *Proc. Natl. Acad. Sci. USA* **103**, 18332-18337.
van de Bospoort, R., Farina, M., Schmitz, S. K., de Jong, A., de Wit, H., Verhage, M. and Toonen, R. F. (2012). Munc13 controls the location and efficiency of dense-core vesicle release in neurons. *J. Cell Biol.* **199**, 883-891.
van den Pol, A. N. (2012). Neuropeptide transmission in brain circuits. *Neuron* **76**, 98-115.
Washbourne, P., Thompson, P. M., Carta, M., Costa, E. T., Mathews, J. R., Lopez-Bendito, G., Molnar, Z., Becher, M. W., Valenzuela, C. F., Partridge, L. D. et al. (2002). Genetic ablation of the t-SNARE SNAP-25 distinguishes mechanisms of neuroexocytosis. *Nat. Neurosci.* **5**, 19-26.

Journal of Cell Science (2017) 130, 1877-1889 doi:10.1242/jcs.201889

Weber, J. P., Toft-Bertelsen, T. L., Mohrmann, R., Delgado-Martinez, I. and Sørensen, J. B. (2014). Synaptotagmin-7 is an asynchronous calcium sensor for synaptic transmission in neurons expressing SNAP-23. *PLoS ONE* **9**, e114033.

Wierda, K. D. B., Toonen, R. F. G., de Wit, H., Brussaard, A. B. and Verhage, M. (2007). Interdependence of PKC-dependent and PKC-independent pathways for presynaptic plasticity. *Neuron* **54**, 275-290.

Wong, M. Y., Zhou, C., Shakiryanova, D., Lloyd, T. E., Deitcher, D. L. and Levitan, E. S. (2012). Neuropeptide delivery to synapses by long-range vesicle circulation and sporadic capture. *Cell* **148**, 1029-1038.

Zhai, R. G., Vardinon-Friedman, H., Cases-Langhoff, C., Becker, B., Gundelfinger, E. D., Ziv, N. E. and Garner, C. C. (2001). Assembling the presynaptic active zone: a characterization of an active zone precursor vesicle. *Neuron* **29**, 131-143.

Supplementary Figures

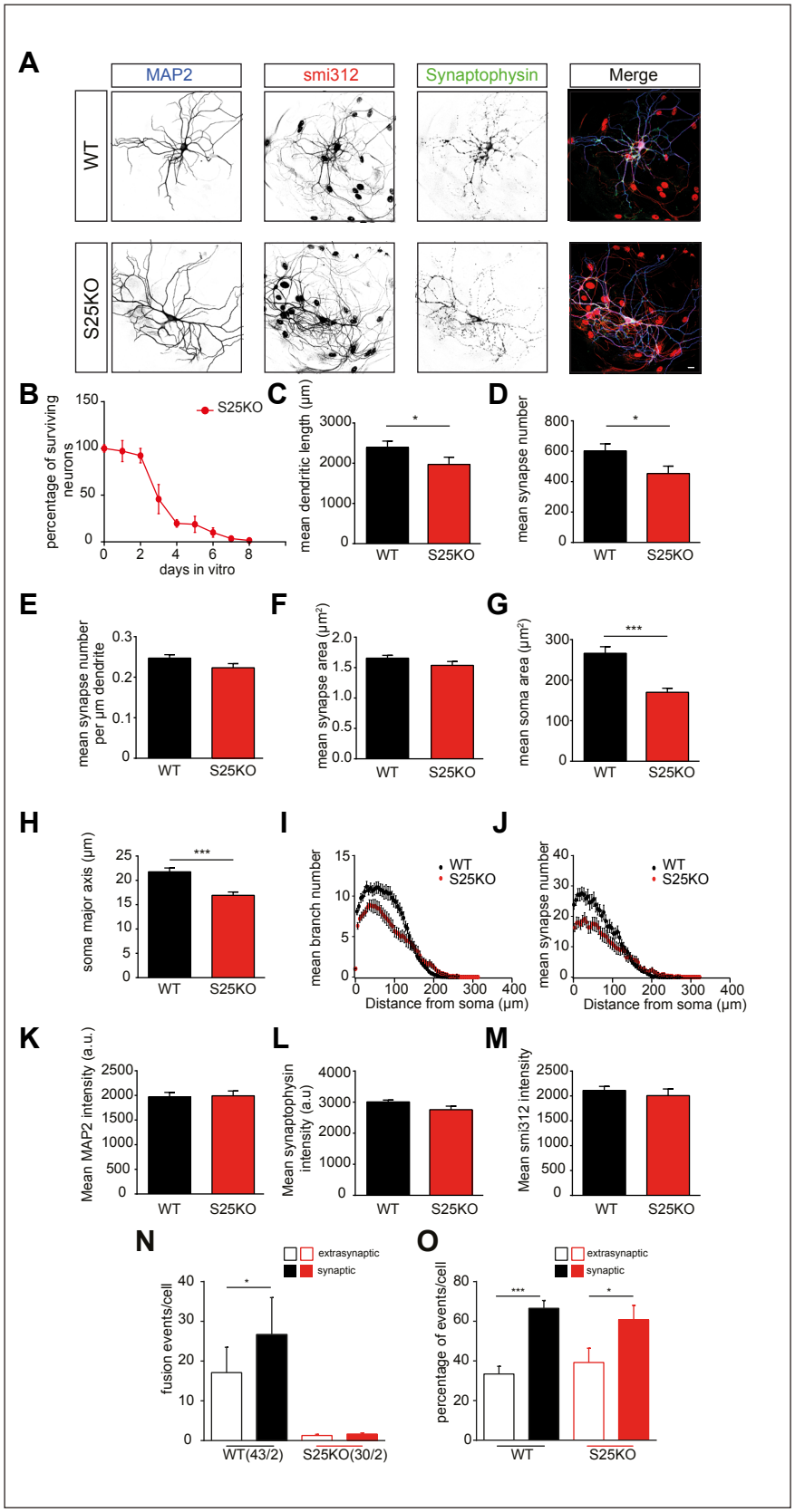

Supplementary Figure 1 Deletion of SNAP-25 reduces neuronal survival, dendrite length and arborization at DIV14 but does not affect localization of remaining DCV fusion events

(A) Representative images of DIV14 WT and SNAP-25 KO (S25KO) neurons stained for dendritic marker MAP2 (blue), axonal marker smi312 (red) and synapse marker synaptophysin (green). Scale bar, 10 μm.

(B) Survival curve showing percentage of surviving S25KO neurons from the day of plating (DIV0) over the subsequent 8 days in vitro. On average ±1% of S25KO neurons survives till DIV8.

(C) Mean dendritic length of WT and S25KO neurons (MW * $p = 0.025$).

(D) Mean synapse number of WT and S25KO neurons (MW * $p = 0.018$).

(E) Mean synapse number per μm dendrite of WT and S25KO neurons (MW * $p = 0.117$).

(F) Mean synapse area of WT and S25KO neurons (MW $p = 0.121$).

(G) Mean soma area of WT and S25KO neurons (MW *** $p < 0.0001$).

(H) Soma major axis of WT and S25KO neurons (MW *** $p < 0.0001$).

(I) Sholl analysis of mean number of dendrites with increasing distance from the soma of WT and S25KO neurons.

(J) Sholl analysis of mean number of synapses with increasing distance from the soma of WT and S25KO neurons.

(K) Mean MAP2 intensity of WT and S25KO neurons (MW $p = 0.749$).

(L) Mean synaptophysin intensity of WT and S25KO neurons (MW $p = 0.267$).

(M) Mean smi312 intensity of WT and S25KO neurons (MW $p = 0.536$).

n/N for C-M: WT: 49/3 and S25KO: 44/3

(N) Extra-synaptic and synaptic DCV fusion events in WT and S25KO neurons (WT: n = 43 cells, N = 2, 1882 events, MW * p = 0.013; S25KO: n = 30 cells, N = 2, 89 events).

(O) Percentage of extra-synaptic and synaptic fusion events in WT and S25KO neurons (WT: MW *** p < 0.0001; S25KO: MW * p = 0.04).

Data is plotted as mean ± SEM.

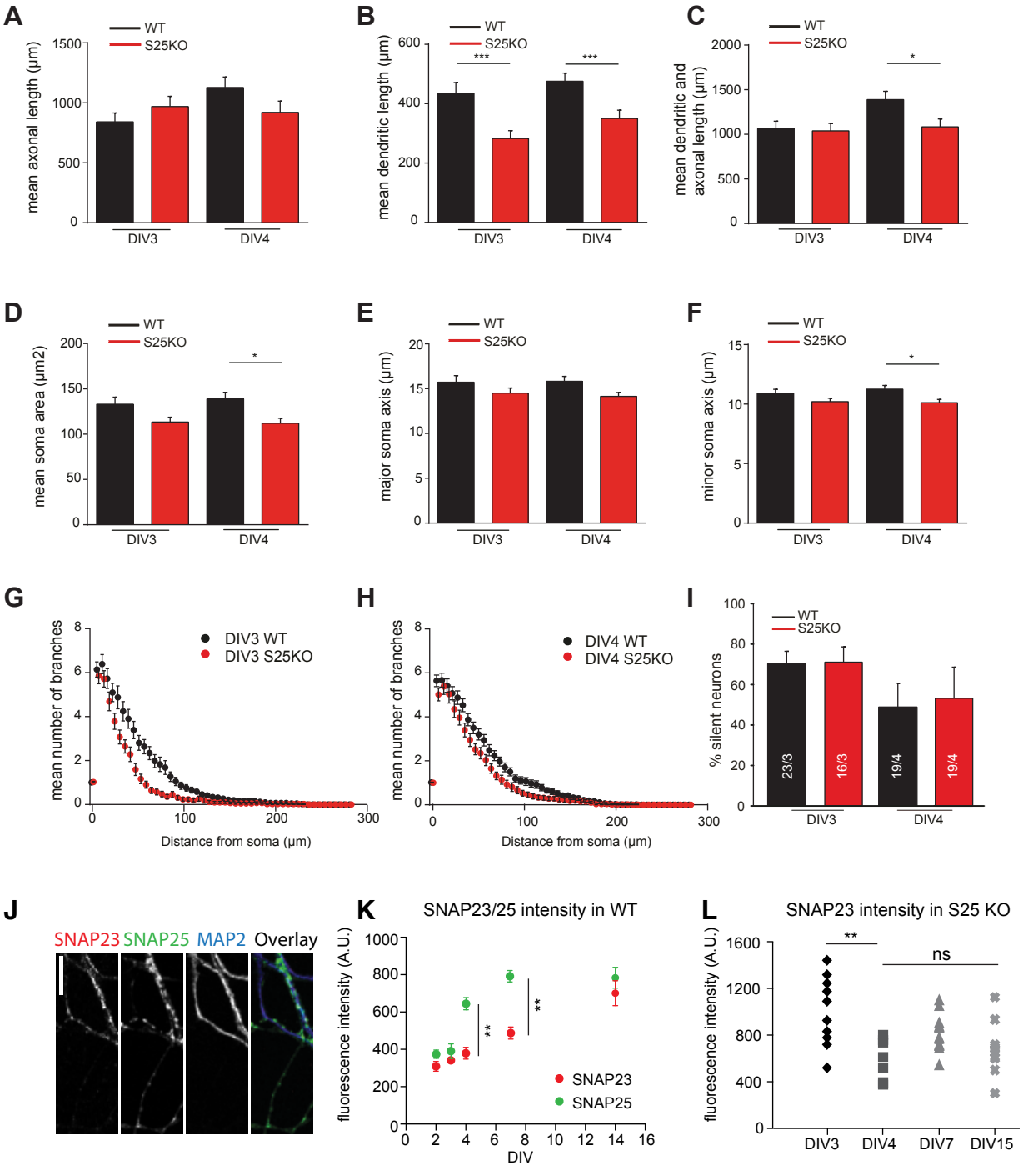

Journal of Cell Science • Supplementary information

Supplementary Figure 2 SNAP-25 KO neurons are smaller compared with control at DIV3 and DIV4

(A) Mean axonal length of DIV3 and -4 WT and S25KO neurons (DIV3 MW p = 0.3148, DIV4 MW p = 0.086).

(B) Mean dendritic length of WT and S25KO neurons (DIV3 MW *** p = 0.0008, DIV4 MW *** p = 0.0003).

(C) Mean dendritic and axonal length of WT and S25KO neurons (DIV3 MW p = 0.723, DIV4 MW * p = 0.014).

(D) Mean soma area of WT and S25KO neurons (DIV3 MW p = 0.0739, DIV4 MW * p = 0.012).

(E) Soma major axis of WT and S25KO neurons (DIV3 MW p = 0.1756, DIV4 MW p = 0.055).

(F) Soma minor axis of WT and S25KO neurons (DIV3 MW p = 0.184, DIV4 MW * p = 0.017).

(G) Sholl analysis of mean number of dendrites with increasing distance from the soma of DIV3 WT and S25KO neurons.

(H) Sholl analysis of mean number of dendrites with increasing distance from the soma of DIV4 WT and S25KO neurons.

n/N for (A- H): DIV3 WT: 64/3 and S25KO: 57/3. DIV4 WT: 42/3 and S25KO: 42/3

(I) Percentage of S25KO and WT neurons unresponsive to electrical stimulation (silent neurons) (DIV3 MW p = 0.90, DIV4 MW p = 0.77). n/N : DIV3 WT: 23/3 and S25KO: 16/3. DIV4 WT: 19/4 and S25KO: 19/4.

(J) Typical confocal images of DIV4 WT neuron stained for SNAP23 (red), SNAP25 (green) and the dendritic marker MAP2. Scale bar represents 10 µm.

(K) Fluorescence intensity of endogenous SNAP-23 or SNAP-25 in soma of WT neurons measured at DIV2, 3, 4, 7 and DIV14 shows increase in expression levels of both proteins and indicates a sharp increase in SNAP-25 expression between DIV3-4 (n = 10 cells per DIV). ** $p < 0.001$.

(L) Fluorescence intensity of SNAP-23 in SNAP-25 KO neurons shows significant reduction of SNAP-23 expression between DIV3 and DIV4, coinciding with massive cell loss. SNAP-23 expression in surviving (<1%) SNAP-25 KO neurons remains stable from DIV4 onwards (DIV7 and DIV15). Individual cells are plotted (n = 10 cells per DIV). ** $p = 0.0012$ MW.

Data is plotted as mean ± SEM.

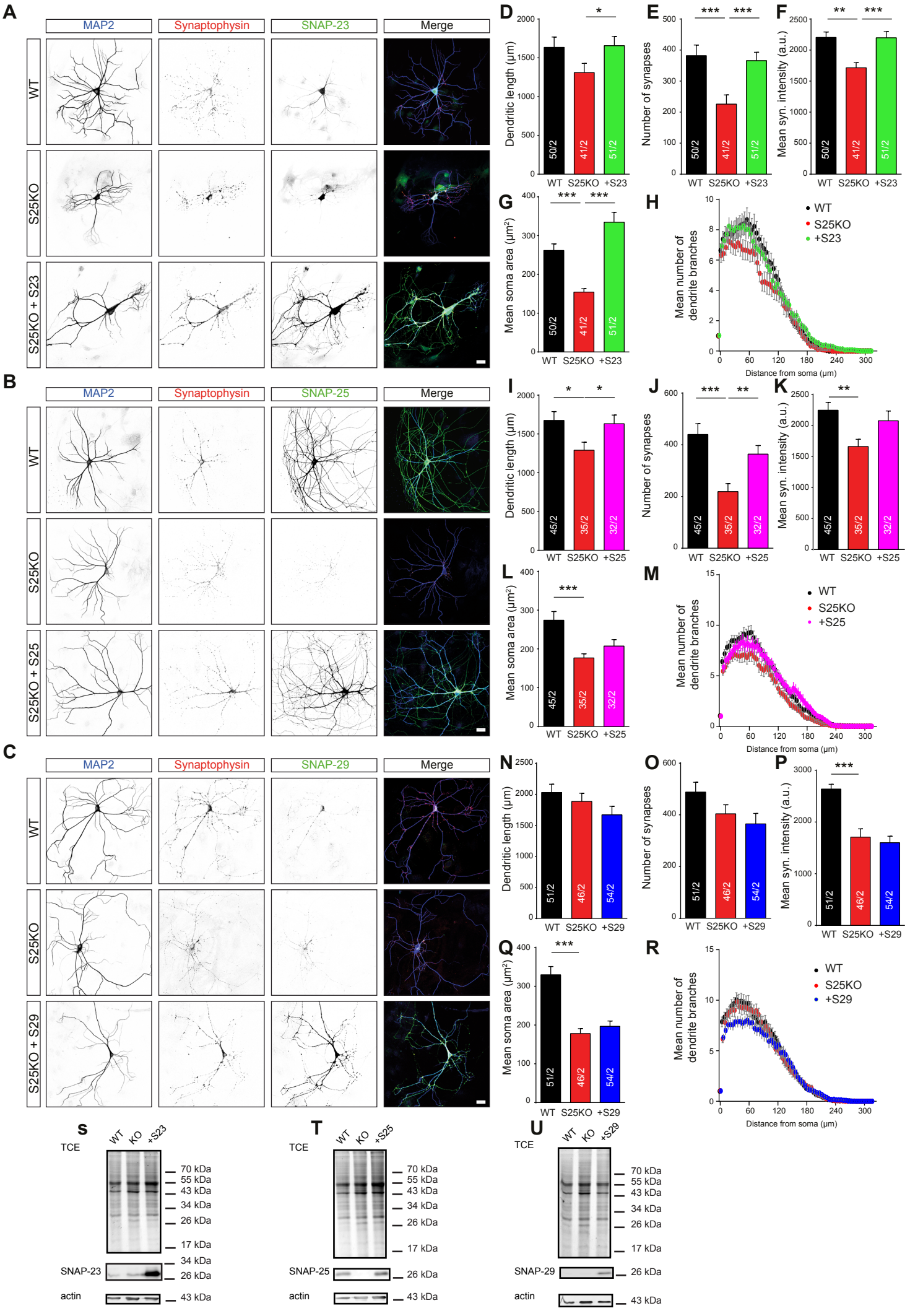

Journal of Cell Science • Supplementary information

Supplementary Figure 3 Rescue of morphological features and localization of endogenous and overexpressed SNAP-23 and -29 in SNAP-25 KO and wild type neurons.

(A) MAP2 (blue), Synaptophysin (red) and SNAP-23 (green) in wild type WT, S25KO and S25KO neurons expressing SNAP-23.

(B) MAP2 (blue), Synaptophysin (red) and SNAP-25 (green) in wild type WT, S25KO and S25KO neurons expressing SNAP-25.

(C) MAP2 (blue), Synaptophysin (red) and SNAP-29 (green) in wild type WT, S25KO and S25KO neurons expressing SNAP-29.

(D,I,N) Dendritic lengths of SNAP-23, 25 and 29 rescued neurons compared to WT and S25KO neurons.

(E,J,O) Number of synapses of SNAP-23, 25 and 29 rescued neurons compared to WT and S25KO neurons.

(F,K,P) Synaptophysin intensity of SNAP-23, 25 and 29 rescued neurons compared to WT and S25KO neurons.

(G,L,Q) Mean soma area of SNAP-23, 25 and 29 rescued neurons compared to WT and S25KO neurons.

(H,M,R) Sholl analysis of mean number of dendrite branches of SNAP-23, 25 and 29 rescued neurons compared to WT and S25KO neurons.

Data is plotted as mean ± SEM.

(S) Western blot of cultured WT, surviving S25KO neurons and S25KO neurons expressing SNAP-23 stained for SNAP-23 and actin.

(T) Western blot of cultured WT, surviving S25KO neurons and S25KO neurons expressing SNAP-25 stained for SNAP-25 and actin.

(U) Western blot of cultured WT, surviving S25KO neurons and S25KO neurons expressing SNAP-29 stained for SNAP-29 and actin.

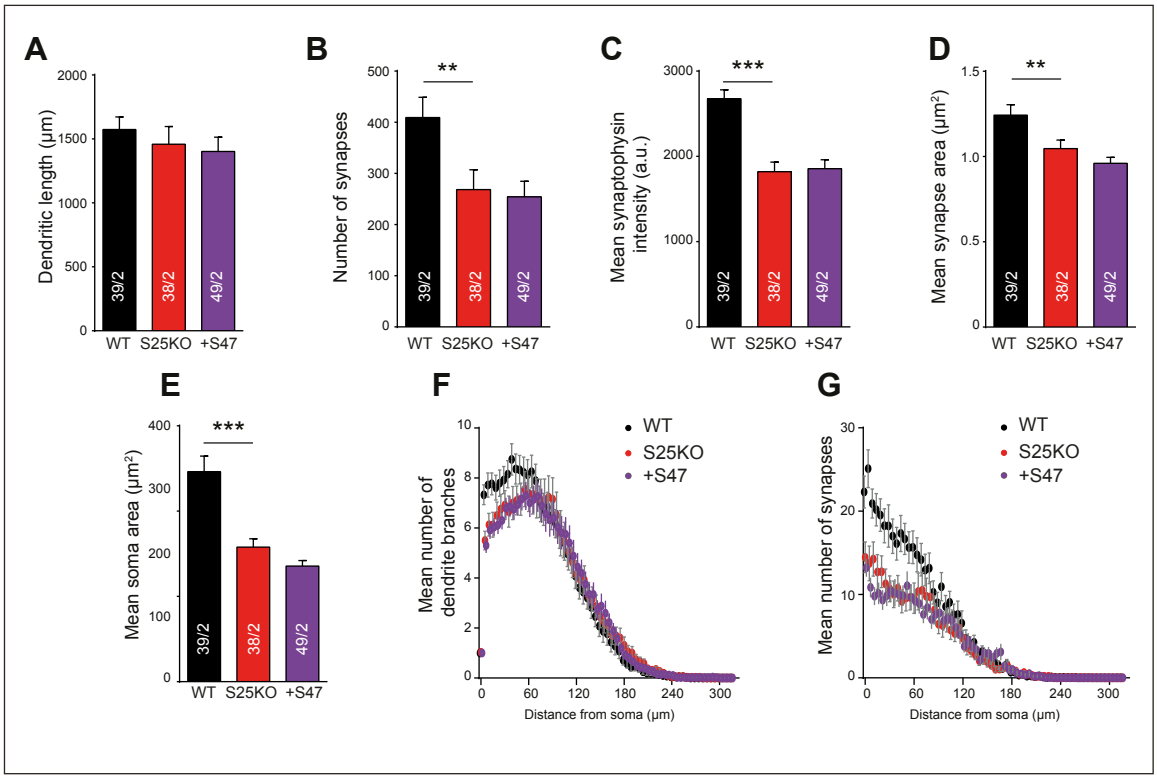

Supplementary Figure 4 Viral expression of SNAP-47 does not rescue morphological defects of SNAP-25 KO neurons

(A) Dendritic lengths of WT, S25KO and S25KO neurons rescued with SNAP-47.

(B) Number of synapses of WT, S25KO and S25KO rescued with SNAP-47.

(C) Synaptophysin intensity of WT, S25KO and S25KO rescued with SNAP-47.

(D) Mean synapse area of WT, S25KO and S25KO rescued with SNAP-47.

(E) Mean soma area of WT, S25KO and S25KO rescued with SNAP-47.

(F) Sholl analysis of mean number of dendrite branches of WT, S25KO and S25KO rescued with SNAP-47.

(G) Sholl analysis of mean number of synapses of WT, S25KO and S25KO rescued with SNAP-47.

Data is plotted as mean ± SEM.